Istituto di Fisica del Plasma "Piero Caldirola" Consiglio Nazionale delle Ricerche

KTH VETENSKAP OCH KONST

ENEA ITALIAN NATIONAL AGENCY FOR NEW TECHNOLOGIES, ENERGY AND SUSTAINABLE ECONOMIC DEVELOPMENT

Magnetic dust mobilization in FTU.

M.De Angeli, E. Lazzaro, P. Tolias, S. Ratynskaia, M.L. Apicella, C. Castaldo, G. Daminelli, G. Gervasini, G. Giacomi, E. Giovannozzi, G. Granucci, M. Iafrati, D. Iraji, S. Lecci, G. Maddaluno, G. Riva, A. Uccello, L. Vignitchouk.

May 29th, 2018

ICMATE Consiglio Nazionale delle Ricerche - CNR Istituto di Chimica della Materia Condensata e di Tecnologie per l'Energia

Amirkabir University of Technology

Layout of the presentation

- BACKGROUND aspects about magnetic dust in tokamaks;
- EXPERIMENTAL PROCEDURE;
- EVIDENCE of the presence of dust lifted up *prior to* the beginning of discharges;
- DISCUSSION on the experimental evidence;
- EVALUATION of the possible impacts of the presence of flying dust *prior to* the beginning of discharges in tokamaks;
- CONCLUSIONS

Background

- **Magnetic dust has already been observed in tokamaks** (Globus-M ~10 wt%, Textor ~15 wt%, Alcator C-Mod, DIII-D) and in particular in FTU ~30 wt% [1].

To date:

- Dust dynamic has been studied **only during plasma discharges** (exception: in DIII-D they accidently observed, in one occasion, dust moving in the vessel 300ms *prior to* plasma, no clear explanation [2]).
- Dust is believed to be **lifted up and mobilized only by plasma** drag forces or by severe thermal shocks.
- **Nobody takes into account** dust presence *prior to* the formation of a proper plasma discharge.
- Previous hypothesis: **possible effects of the presence of dust during the plasma start-up** have been proposed by J. Winter [3,4] since 1998.

[1] M. De Angeli, L. Laguardia, G. Maddaluno, et al., Nucl. Fusion 55 (2015) 123005.
[2] D.L. Rudakov, A. Litnovsky, et al., Nucl. Fusion 49 (2009) 085022.
[3] J. Winter, Plasma Phys. Control. Fusion 40 (1998) 1201.
[4] J. Winter, Phys. Plasmas 7 (2000) 3862.

Experimental layout

- **TS** (Port 11) dust signal acquired during *Zero*-discharges and with anticipated trigger at -0.5s;
- **IR camera** (port 1 up) dust images acquired with anticipated trigger at -2s;
- **Exposure of samples** with pre-deposited magnetic dust during *zero*-discharges;
- **Dust collection** during *zero discharges*.

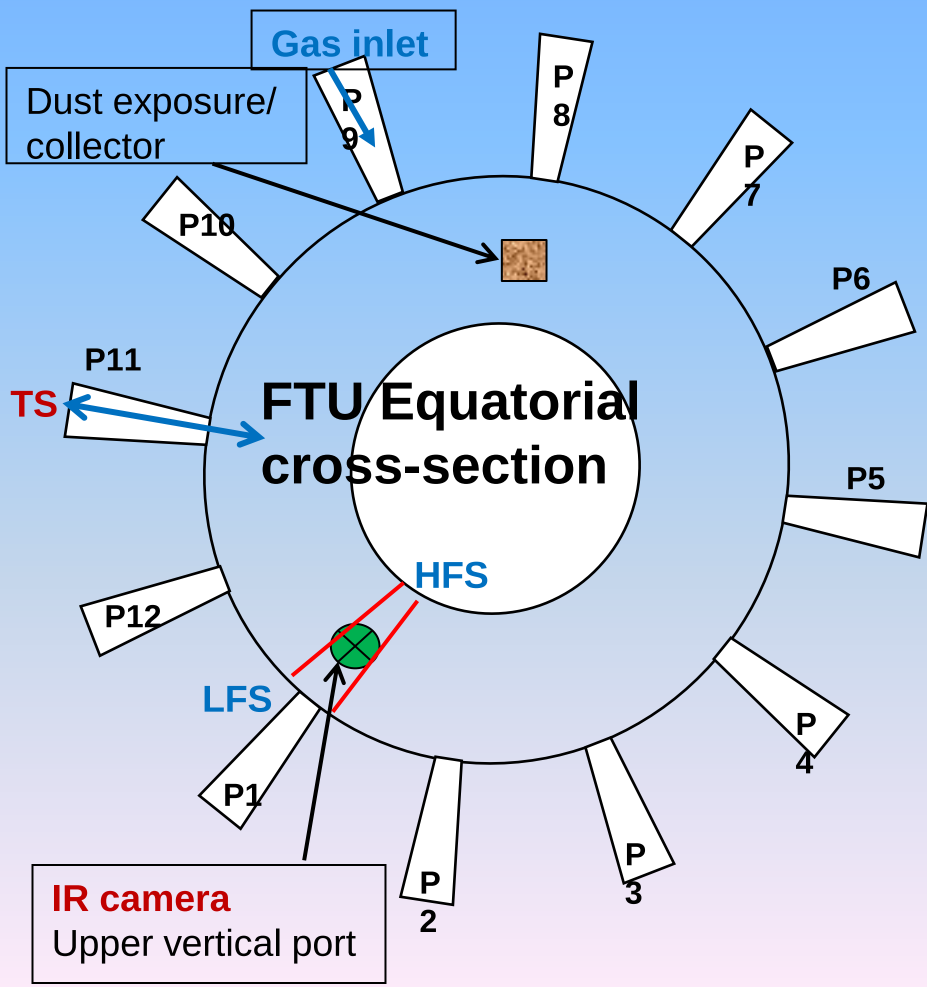

Volumes of sight of TS spectrometers (FTU poloidal cross-section):

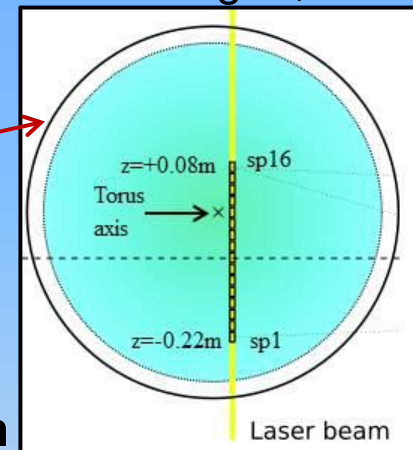

View field of IR camera mounted on the upper vertical port 1:

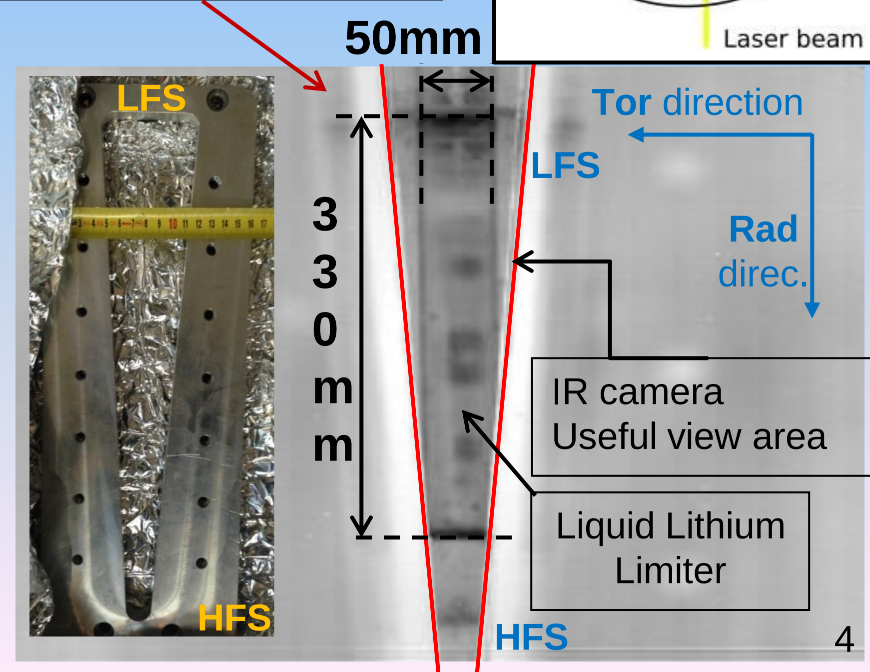

Evidence of the presence of mobilised dust, *prior to* plasma discharges, in FTU

TS spectra acquired during *zero*-discharges

(~20% events found over 597 *zero*-discharges analysed between 2007 and 2015)

A) Shot# 36970, Ch0, Sp11, B_t=7.6T

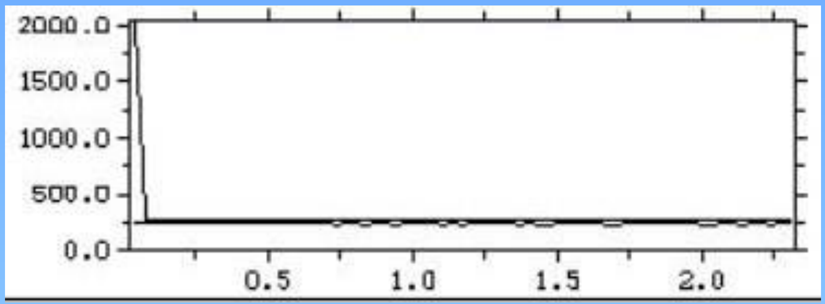

B) Shot#38539, Ch0, Sp8, B_t=5.2T, $t_{plateau}$=1.5s

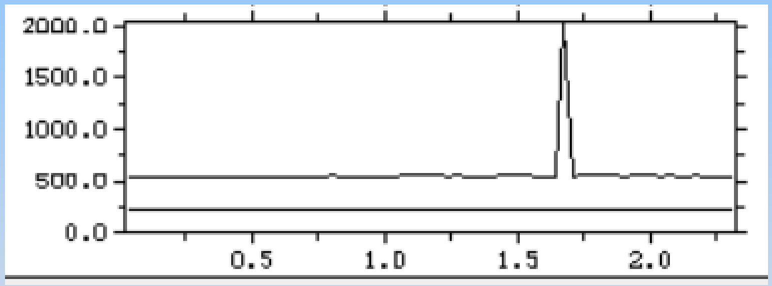

C) Shot# 36001, Ch0, Sp7, B_t=6T, $t_{plateau}$=1.5s

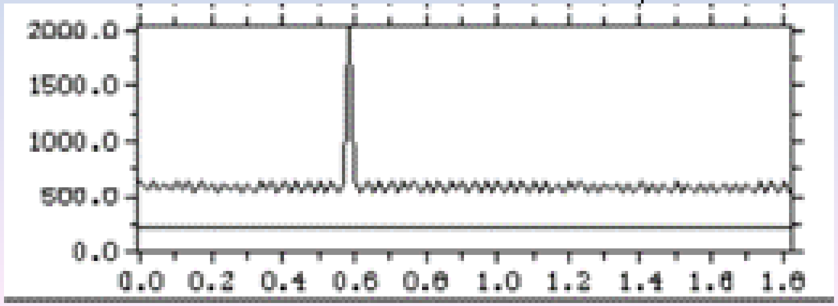

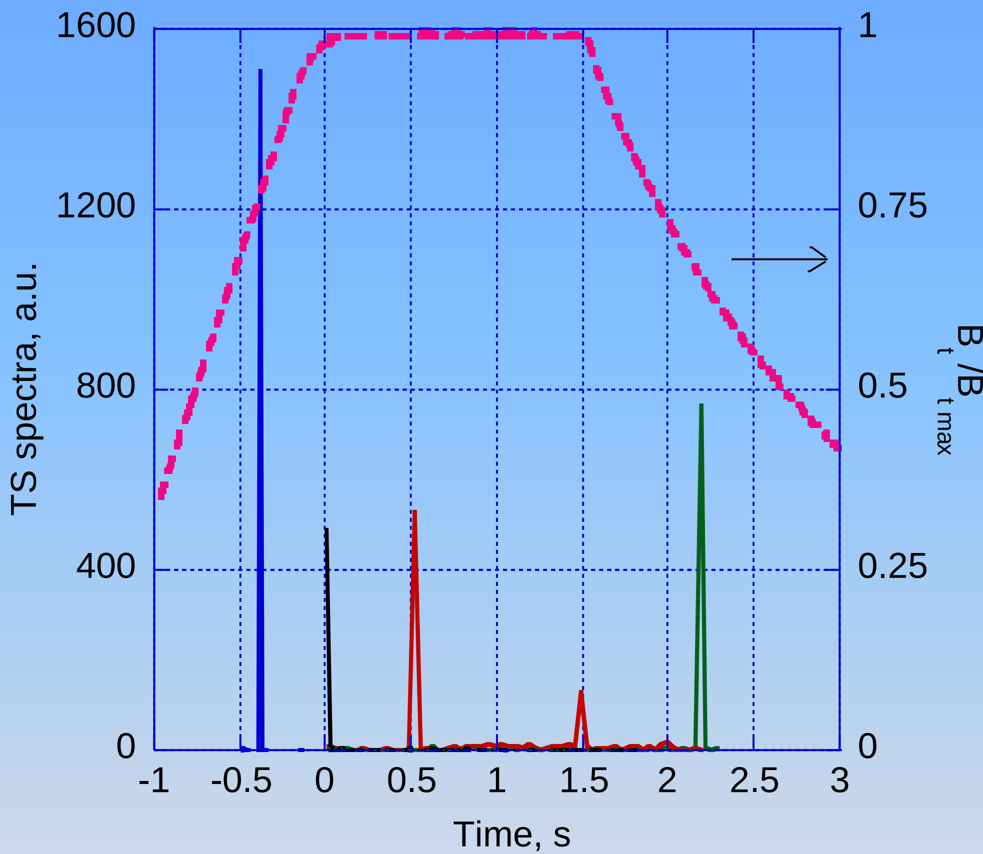

TS spectra showing the presence of <u>dust in *Zero*-discharges</u> (**black**, **red** and **green** peaks) and <u>*prior to* plasma discharges</u> (**blue** peak).

TS spectra, anticipated trigger @ -0.5s

(5 events found over 114 discharges acquired)

A) Shot# 40713 (Soft Stop RE), Ch 0, Sp 4.

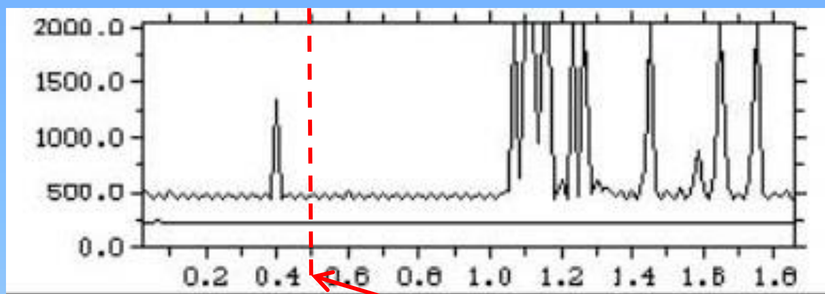

B) Shot# **40737** (disr @0.46s), Ch 0, Sp 8 (see next slide and IR cam. summary).

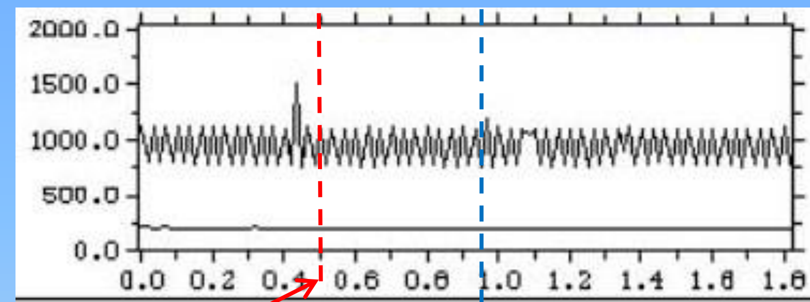

t=0 plasma discharge

C) Shot# 40780 (disr @0.3s), Ch 0, Sp 6.

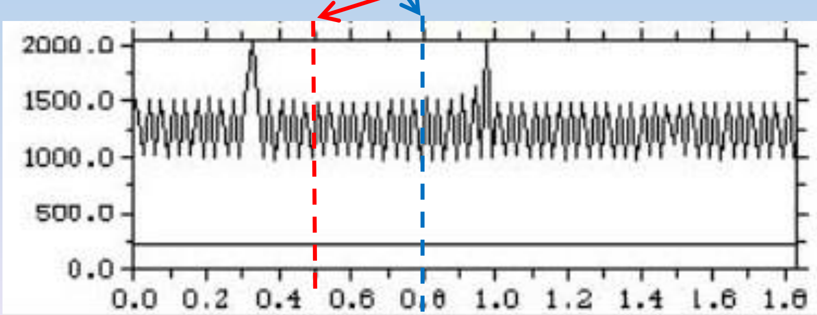

D) Shot# 40792 (disr @0.5s), Ch 0, Sp 5.

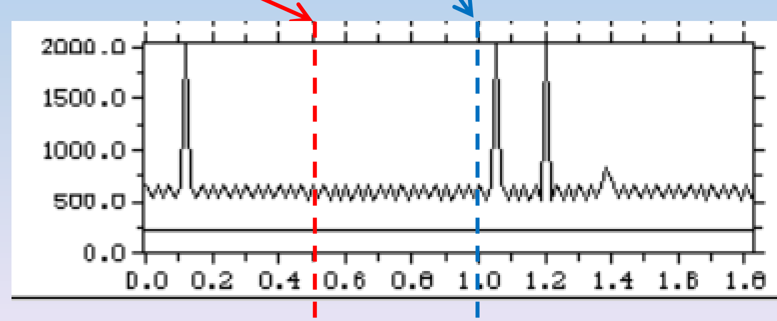

Example of post-processed TS spectra

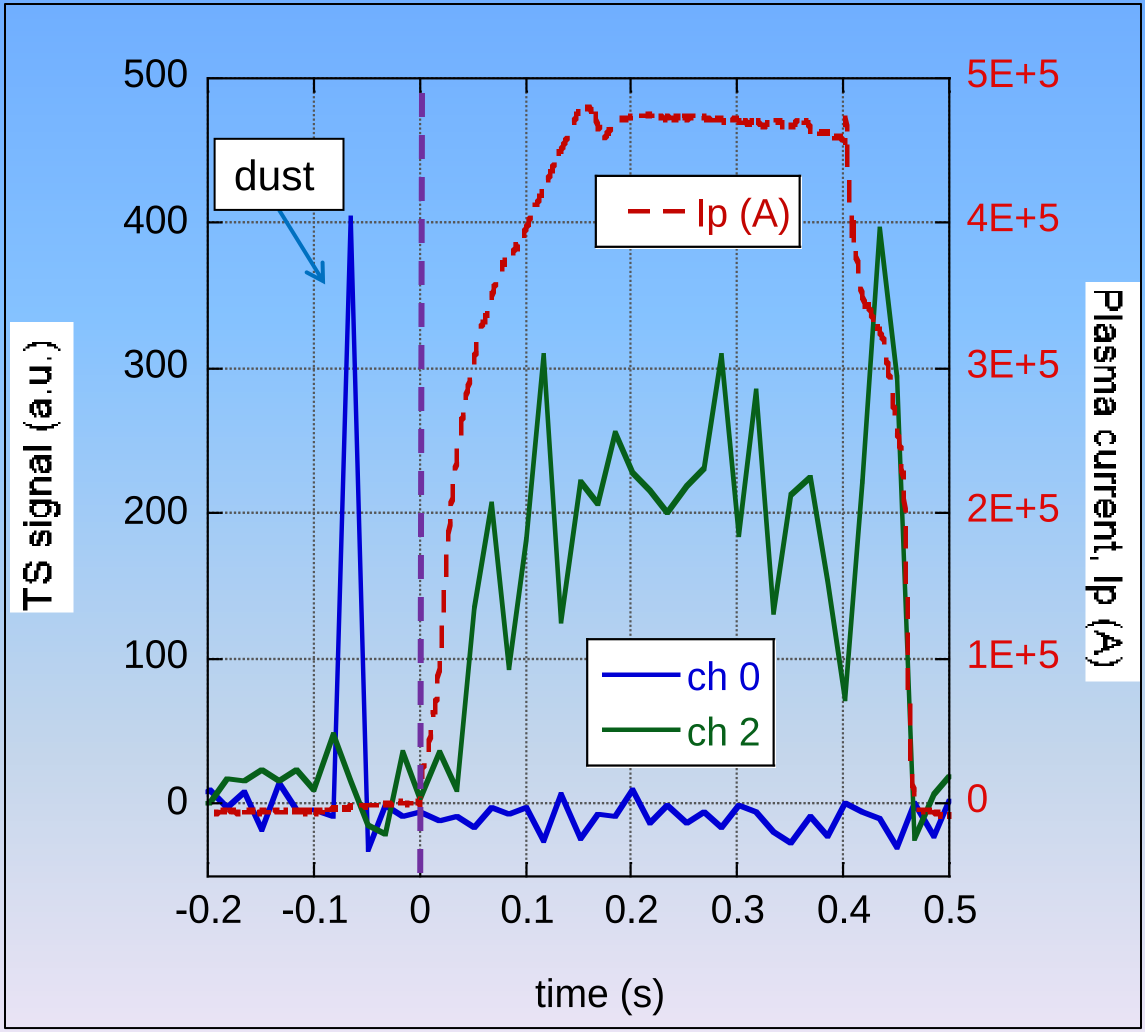

Dust grain remobilized *prior to* the beginning of the plasma discharge in shot #40737 (disruption at t = 0:46s), B_t at plateau 4T.

Ch 0: laser wavelenght;
Ch 2: shifted wavelenght (i.e. proportional to plasma density).

Estimated dust density by TS

Experimental campaign	# *Zero*-disc analysed	# *Zero*-disc with dust	% of *Zero*-disc with dust	Estimated dust density, cm^{-3}
F07 (1)	3	2	-	-
S08 (1)	3	2	-	-
F08	14	1	7.1%	5.3E-03
S09	82	13	15.9%	8.2E-03
F09	34	7	20.6%	6.6E-03
S10	16	6	37.5%	2.8E-02
F10 (1)	7	2	28.6%	1.8E-02
S11	79	27	34.2%	1.9E-02
F11	TS not	available	-	-
S12	18	1	5.6%	2.2E-03
F12	82	12	14.6%	5.9E-03
S13	TS not	available	-	-
F13	79	24	30.4%	1.6E-02
S14	53	13	24.5%	1.5E-02
F14	27	1	3.7%	1.9E-03
S15	100	12	12%	6.6E-03
F15	TS not	available	-	-
Total:	597	123	20.6%	

(1) = TS not available for several *Zero*-discharges.

Dust density [5]:

$$N_d = \frac{N_{grains}}{N_s N_{las} V_{TS}} \sim 10^{-3} - 10^{-2}\ cm^{-3}$$

N_{grains}: total dust grains detected;
N_s: total discharges analysed;
N_{las}: laser shots per discharge;
V_{TS}: TS volume of scattering ≈ 0.3 cm^3.

Hypotheses for formula applicability:
i) any dust grain in the scattering volume, during a laser shot, is detected;
ii) dust is uniformly present in the whole chamber volume.

Discharges with TS trigger at t= -0.5 s:

Disch Analysed in 2016	# disch with dust	Estimated dust density, cm^{-3}
114	5	6.9E-03

[5] W.P. West, et al., Plasma Phys. Control. Fusion **48** (2006) 1661.

Dust in IR camera images, trigger @ t=-2s

FLIR SC7500 with a **resolution ~ 1.6 mm/px**.

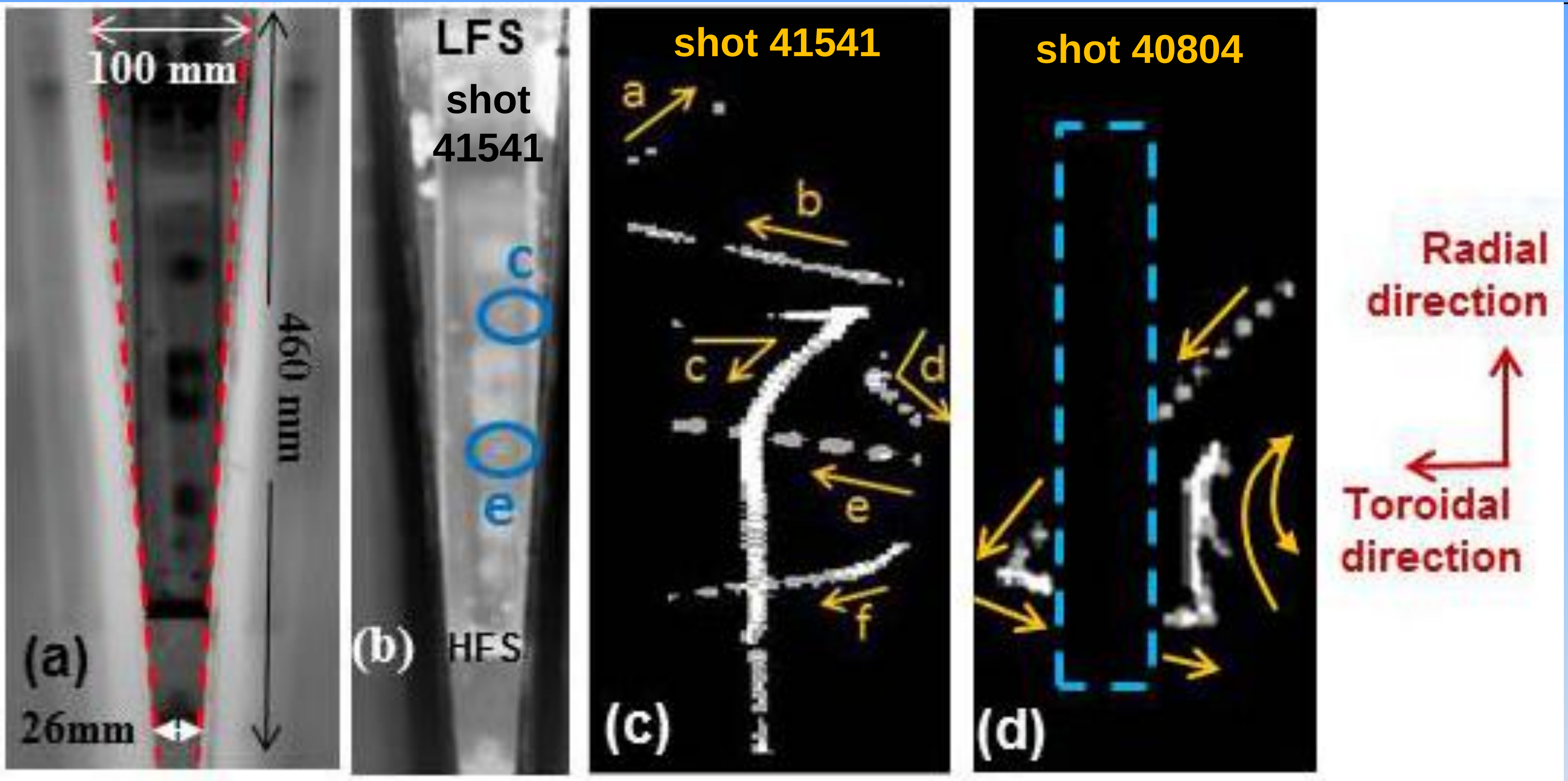

Examples of dust remobilized *prior to* the beginning of discharges. (a) IR-camera view fled inside FTU torus; (b) raw IR camera frame at t =-804.8ms of **shot 41541**; (c) processed frames with 6 grains trajectories in **shot 41541**. Camera rate: 604 frames/s; integration time: 643µs; (d) processed frames showing the **trajectory of a grain entrapped inside the port duct** from t =-840.6ms to t =-343.8ms in **shot 40804**.

IR camera observation, summary table

Numbers of discharges with dust: 14 over 100 analysed (with and w/o warm LLL inserted):

Shot # , dicharge type	Δt dust, ms	B_t , T	2D V_{dust} , m/s	Direction
40688 SS RE	-877 → -872	1.75	16.4	T
40714 Disrupt	-21 → +8	~4	36.9	R
40724 Disrupt	-23 → -18	~4	9.05	T
40726 Disrupt	-3 → +3	~4	10.6	R
40737 Disrupt (IR and TS)	**-13 → +5**	**4.7**	**11.8**	**R**
40801 BrkD	-26	2.95	32.5	T
40803 BrkD	-7→ +22	~4	5.4	T
40804 Disrupt (*) *entrapped*	-840 → -344	1.8-3.33	N/A	N/A
40814 Ok	-1084 → -1066	1.17	0.7	T
40818 Disrupt	-978 → -968	1.4	<<1	T
40819 Ok	-2	4	-	
40990 Ok	-2→ +2	5.3	<<1	R
41541 Disrupt (*) *multi dust*	-877→ -606	2.2-3.2	N/A	N/A
42183 Ok	-1000→ -572	1.7-3.4	~1	R

(*) trajectories shown in previous slide.

Magnetic fields timing

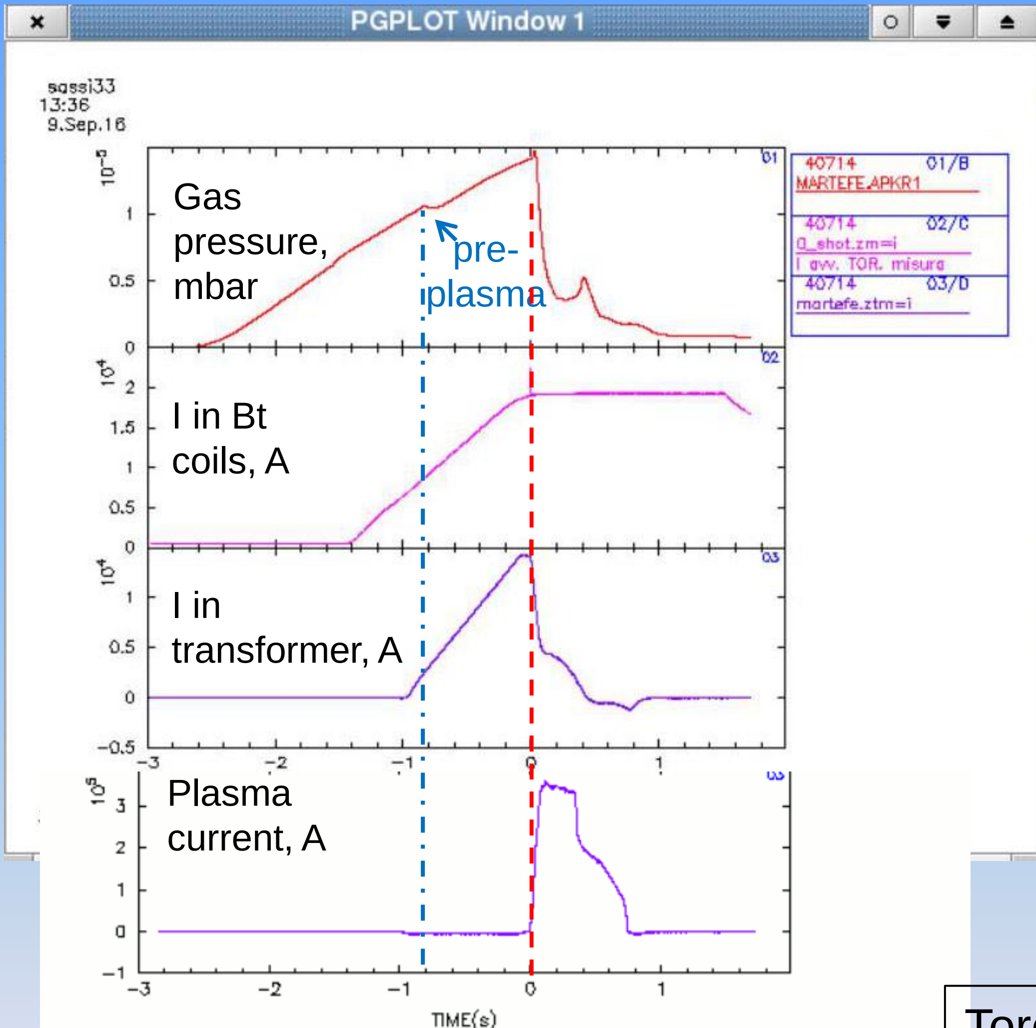

Magnetic field evolution diagram, along with plasma current and neutral gas pressure, for discharge #40714 (disrupted).

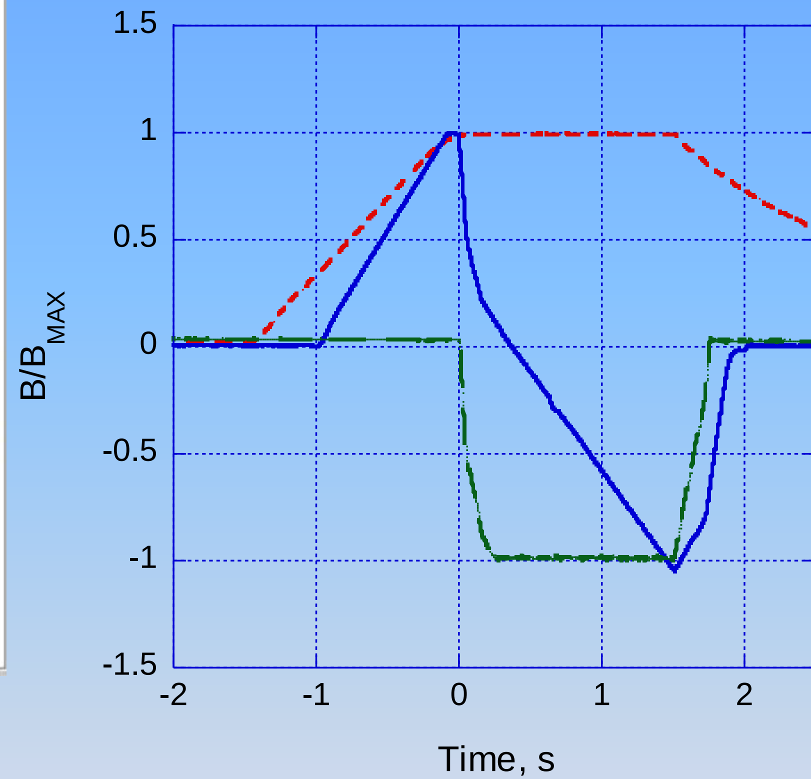

Toroidal magnetic field B_t (red line), ohmic-transformer field B_{trans} (blue line), and vertical field B_v (green line) in a typical FTU plasma discharge. In *Zero*-discharges B_{trans} and B_v are set to zero.

Limiting factors during the investigation

IR camera:

- **Focusing**: particles out of focus are not detected.
- **Thermalized particles**: particles at same temperature than the background are not detected.
- **Shine by «pre-plasma»**: in general, particles are visible after pre-plasma is established (from t~ -1s).

  No particles are visible during pure magnetic discharges (i.e. during *zero*-discharges).
- **Resolution**: the resolution of the IR camera (~1.6 mm/pixel) inhibits the detection of small grains.

TS:

- **Space**: TS acquire signals ONLY if a dust pass through its view volume;
- **Memory limit**: for acquisitions with anticipated trigger;
- **Sampling frequency**: 30Hz for each laser (2 lasers).

Exposure of magnetic dust in *Zero*-discharge

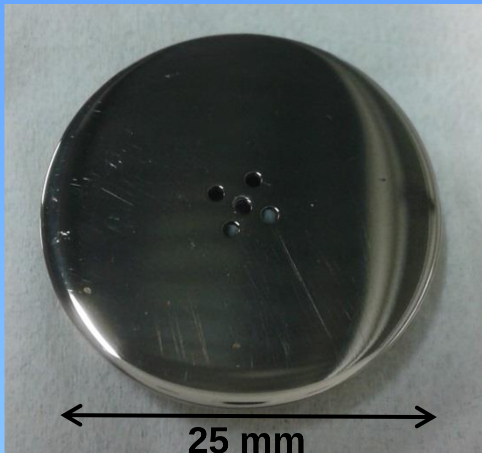

Sample with magnetic dust spots exposed to shots 42176 (Zero) and 42177 (only B_t, B_{trasf}, B_v).

Spots layout

Spots 1-2-3-4: Fe 53 -180 µm (non spherical)
Spot 5 : Mo > 63 µm (spherical)
Spots 6-8 : Fe < 20 µm (non spherical)
Spots 7-9 : W 16 µm (spherical)

Spots 1-2-3-4-5 on the flat bottom of 0.5 mm deep holes; Spots 6-7-8-9 on the sample surface

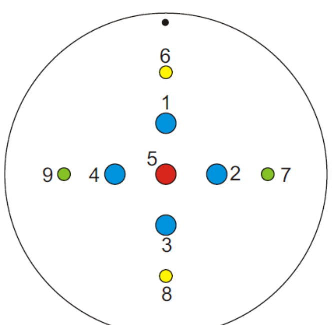

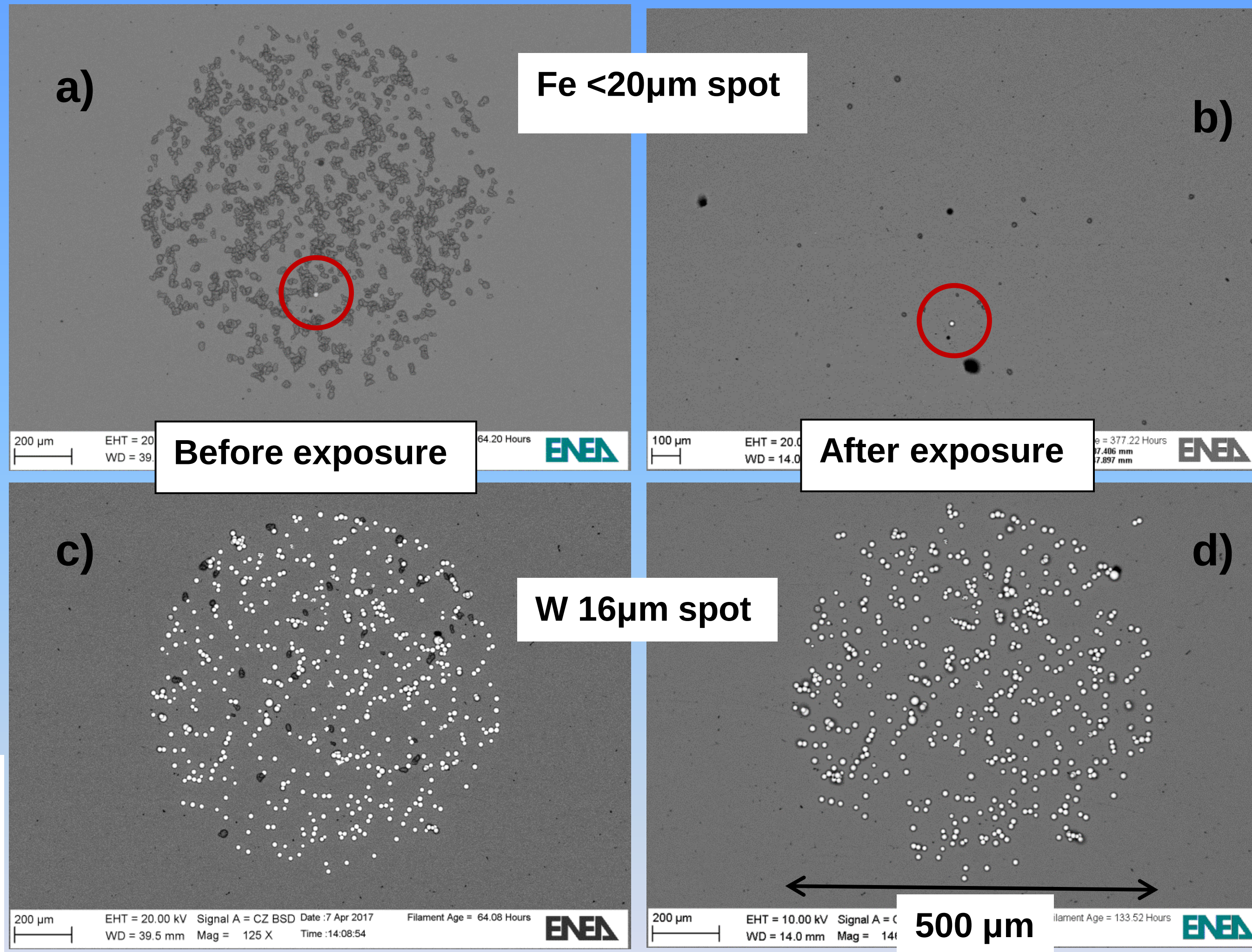

Electron backscattered images of Fe (dark grains) and W (white grains) spots before (a and c) and after (b and d) exposure.

Dust collected during two pure magnetic discharges

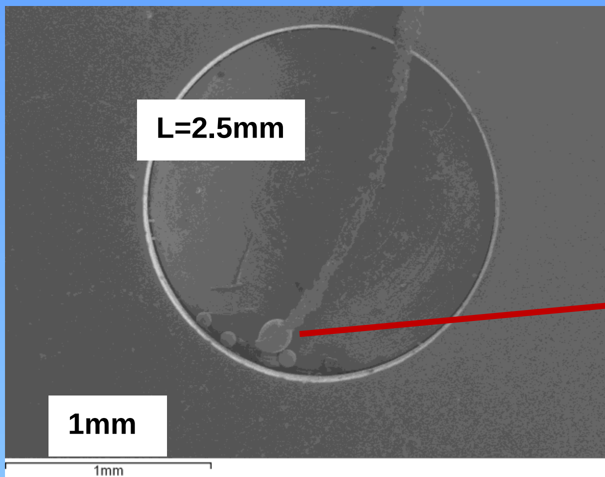

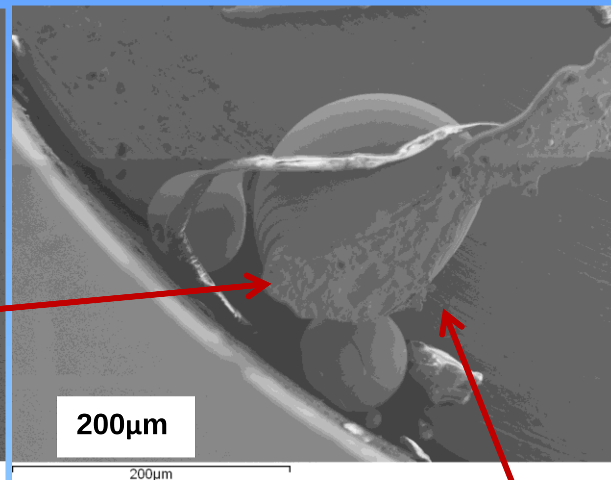

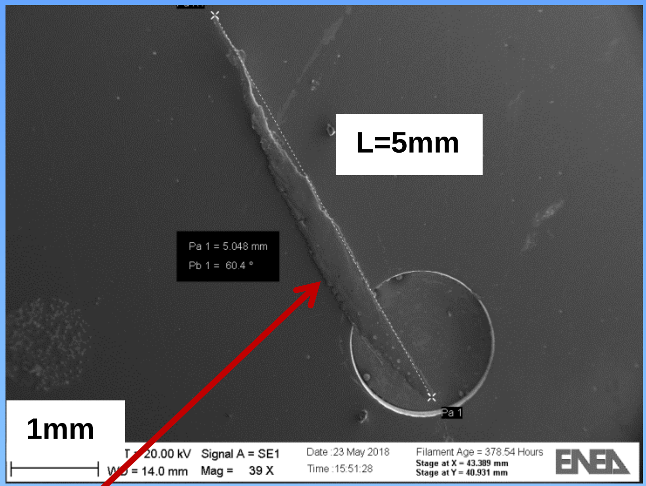

Collection Volume V_{coll}= 330 cm^3;
Average dust density N_d= 10^{-2} cm^{-3};
$\Downarrow$
# of grains expected ~ order of unity!

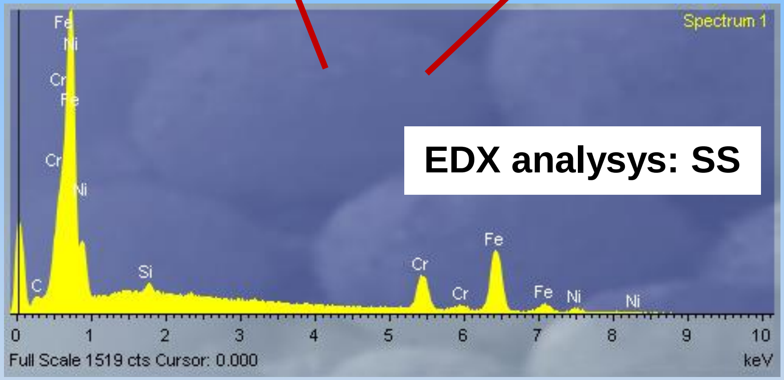

Dust collected in FTU

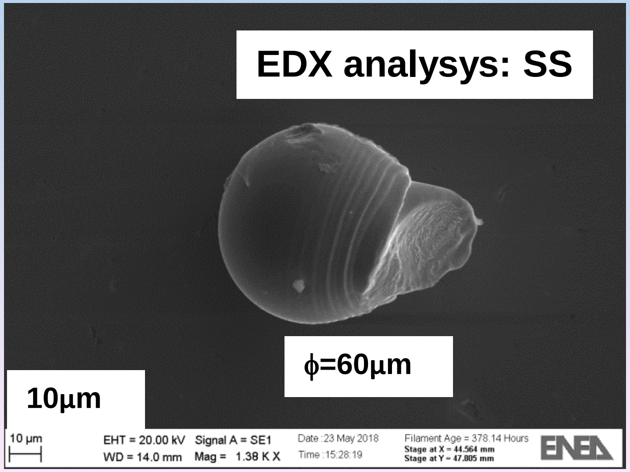

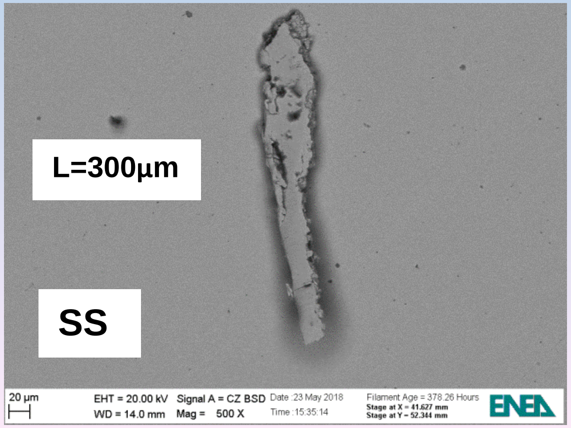

Discussion on the experimental evidence

Vessel vibration

During discharges, the vessel is subject to vibrations. They may induce dust remobilization. The maximum *vertical* acceleration for regular and disrupted discharges has been evaluated. The worst case appears to happen for regular plasma discharges.

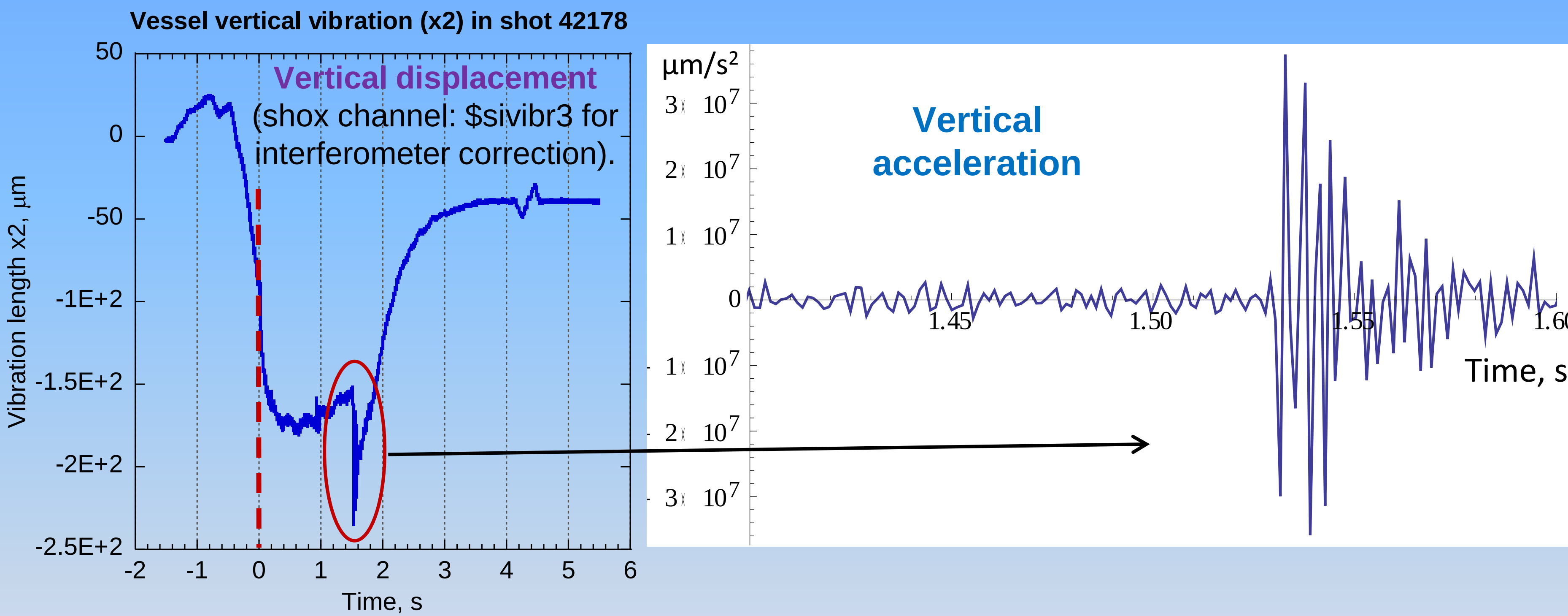

Shot 42178, plasma Ok, B_t=5.3T. Left: vertical vibration displacement (x2); right: magnification between t=1.40-1.60s of the acceleration strength (x2).

The Maximum value of the (vertical) acceleration strength in shot 42178 (Ok discharge) is: ***~16 m/s² ~1.5 g m/s²*** *at the END of the discharge!*

This example well represent FTU vibrations during plasma discharges.

What could lift up and remove dust before discharge?

X **Gas puffing**:

- purified gas filtered by nm size filter; no dust puffed directly into the vessel.
- D_2 gas pressure during pre-fills ~10^{-5} mbar ⇒ m.f.p. $\lambda \approx 10$m, molecular regime!
- dust observed by TS during *zero*-discharges without any gas puffing!

X **Electric field induced by coils during B ramp-up (dI/dt ~15kA/s)**:

- F_E at $E=V_{loop}/L_t$~2-3V/m (*toroidally directed*!) << F_{vdW}, not enough to lift up dust (*e.g.*: $F_{E\ lift\text{-}up}$ 20kV/cm *normal directed* to lifting up spherical dust with D_d ~ 100μm).
- No B_{transf} during *zero*-discharges.

X **Pre-plasma**:

- too weak. No pre-plasma during *zero*-discharges.

X **Vessel vibrations**:

- pulsed force of the order of ***g***, *i.e.* $F_{pulse} \approx F_g < F_{vdW}$ for grains with D_d < 650μm. The higher pulse strength is observed at the end of regular plasma discharges.

✓ **Magnetic field**:

- B field can lift up spherical grains if F_B ($\propto D_d^3$) **>** F_g ($\propto D_d^3$), F_{vdW} ($\propto D_d$); *Example*: for spherical iron grains at B_t~5T ⇒ $F_B > F_{vdW}$ for D_d > 70μm.
- Trapped particle in BEFORE the beginning of the discharge shows a curved trajectory.

⇒ **Only magnetic field force F_B can mobilize dust before plasma discharges!**

Forces strength evaluation for spherical *Fe* grains

Magnetic force:

$\mathbf{F}_B = \boldsymbol{\mu} \cdot \nabla \mathbf{B}$, $\mathbf{B} = B_r(r,z)\mathbf{e}_r + B_\varphi(r)\mathbf{e}_\varphi + B_z(r,z)\mathbf{e}_z \Rightarrow$

$$\begin{cases} F_r = \mu_r \dfrac{\partial B_r}{\partial r} + \mu_z \dfrac{\partial B_r}{\partial z} - \mu_\varphi \dfrac{B_\varphi}{r} \\ F_\varphi = \mu_\varphi \dfrac{B_r}{r} + \mu_r \dfrac{\partial B_\varphi}{\partial r} \\ F_z = \mu_r \dfrac{\partial B_z}{\partial r} + \mu_z \dfrac{\partial B_z}{\partial z} \end{cases}$$

$\mu_r = \mu_\varphi = \mu_z \approx \frac{1}{6}\pi D_d^3 M_{s0} \Rightarrow F_B \propto D_d^3$; $\boldsymbol{\mu}$ magnetic permeability; D_d dust grain diameter; M_{s0} residual magnetisation at 0K.

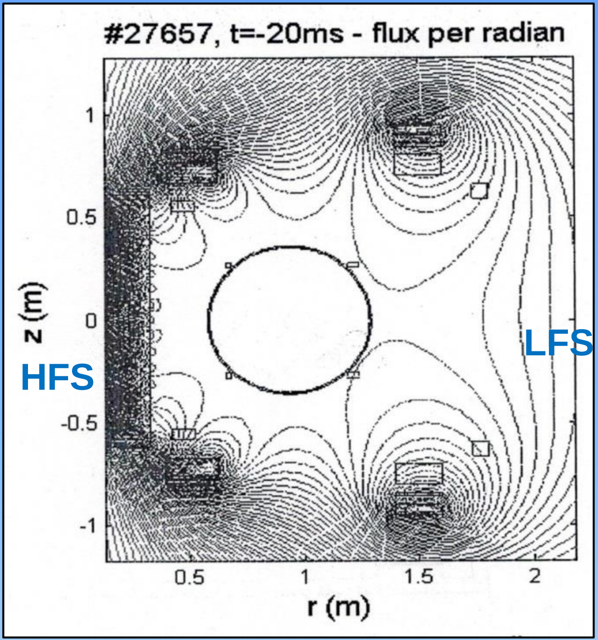

Adhesion force:

Statistical nature depending on the surface roughness; good approssimated by *van der Waals formula* :

$F_{vdW} = \frac{A}{12{z_0}^2} D_d$, A=3.8x10^{-19}J Hamaker constant for *Fe*, z_0=0.4nm.

Gravitational force:

$F_g = m_d g \propto D_d^3$, m_d dust grain mass, g gravitational acceleration.

Example: *Fe* spherical grain D_d=100µm at B_t=5T $\Rightarrow$ **F_B = 3.9µN**; F_{vdW}=1.7µN; F_g=4.1x10^{-2}µN

Forces evaluation

F_g gravitational force; F_{vdW} adhesion force (van der Waals); F_B magnetic force (@ B_t=5T) vs dust diameter for spherical *Fe* grains:

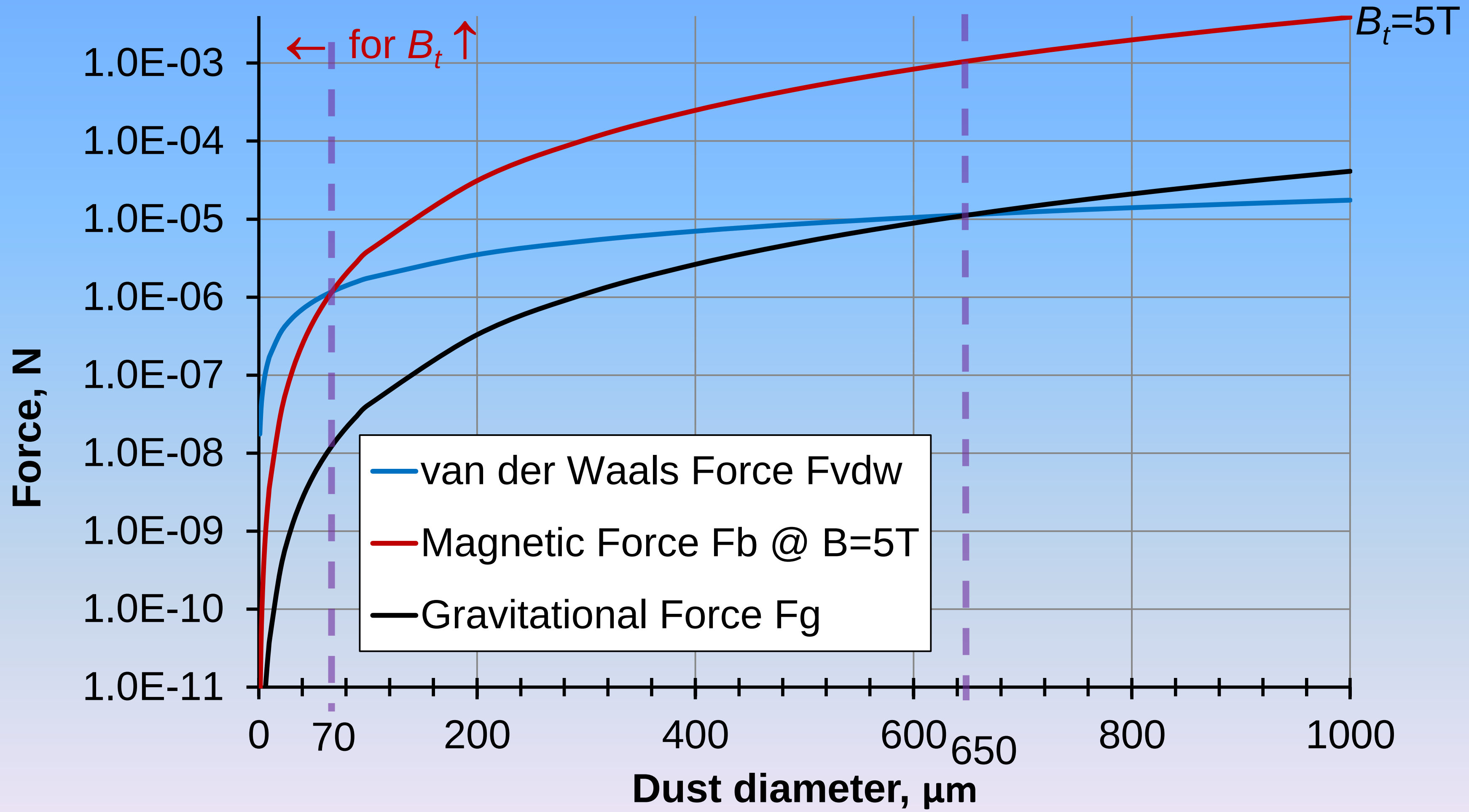

Impact of remobilized dust, *prior to* the beginning of plasma discharges, on tokamaks operations

Breakdown phase

Breakdown by *Townsend* model, rearranged in tokamaks geometry applying *Loeb Meek streamer criterion* [6,7], can describe the electron valance process by the following equation:

$$dN_e = (\alpha - \beta)N_e dx \;\Rightarrow\; N_e = n_0 e^{(\alpha-\beta)x}$$

for uniform coefficients, where α is the primary ionizing collisions coefficient per unit length; β is the attachment collisions coeff., per unit length, on impurity ions or dust.

$$\alpha = A p_g e^{\left(-B p_g / E\right)} \text{ and } \beta = N_d \left\langle \sigma_{e,d} v \right\rangle / u_e$$

where *A,B* are experimental coeff.; *E* is the loop electric field; N_d the dust density.

Example of FTU conditions for a standard discharges:

D_2 gas at $p_g \approx 10^{-3}$ Pa; T_g= 300K; $N_d \sim 10^{-3}$ cm^{-3}, $E \approx$ 1V/m $\Rightarrow$
A= 1.91 m^{-1}Pa^{-1}; *B*= 25.97 V m^{-1}Pa^{-1}

we can draw a gas discharge condition diagram.

[6] A. Pedersen, IEEE Transactions on Power Systems **86(2)** (1967) 200.
[7] L.B. Loeb, J.M. Meek, The Mechanism of the Electric Spark Stanford University Press 1941.

Breakdown phase diagrams

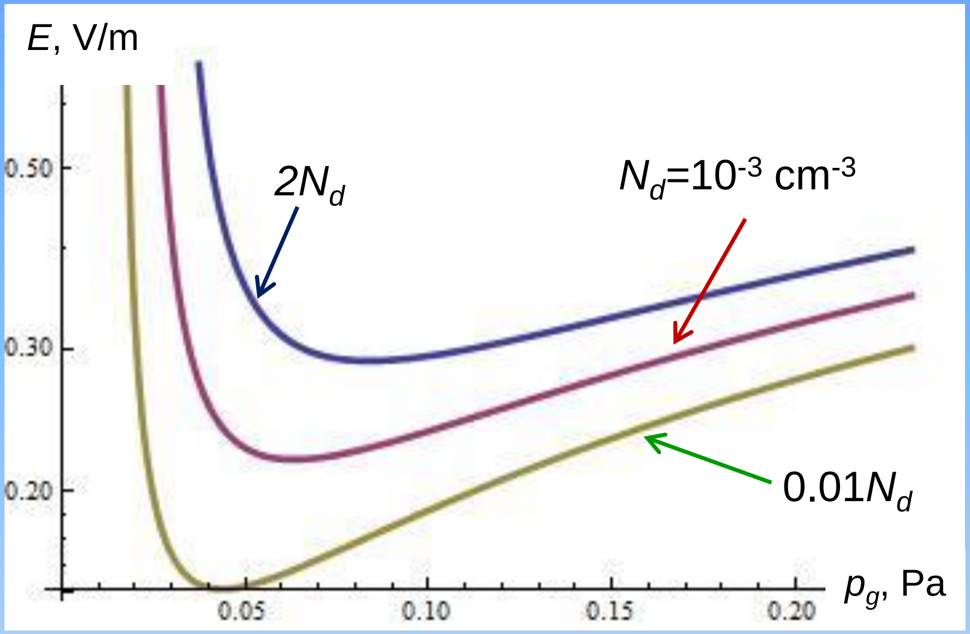

Plot of the breakdown electric field E vs. p_g (Paschen law), with dust effect, at different dust densities.

⇒ The presence of dust affects the electron density (depleting numbers of free electrons) leading to a shift in the Paschen's curve!

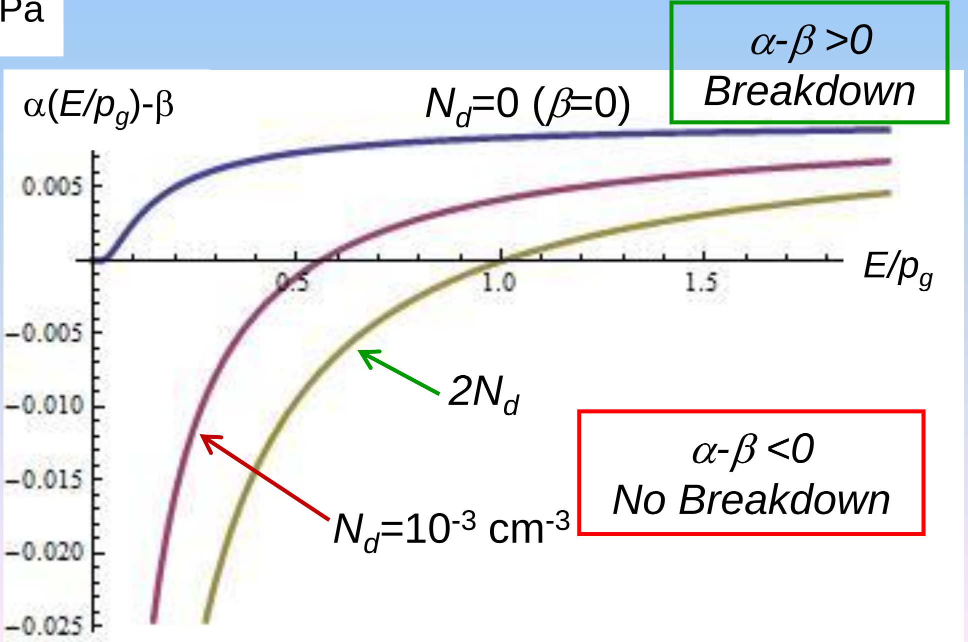

Plot of the effective avalanche rate $\alpha(E/p_g)-\beta$ at different dust densities. The intercept gives the critical E/p_g minimum value for breakdown.

Current ramp-up phase

The physical problem of the transformation from the *avalanche discharge* to the *inductive current rise*, consists in determining the time constant of the transformation, τ_b, and of the corresponding typical value of the current and its scaling with the main parameters of the early discharge state [8]. These parameters depend on the *condition of the avalanche* (Pedersen-Meek condition) and on the *avalanche rate* which is affected by the electron "attachment" rate to dust

$$I_{p<}(t) = I_0\left(e^{\frac{t}{\tau_b}} - 1\right) \quad \text{where} \quad \tau_b^{-1} = (\alpha - \beta)u_e$$

Following the breakdown avalanche stage the relation between the discharge current $I_{p>}(t)$ and the voltage is through a nonlinear resistance and limited by the self-inductance.

$$R = R_0\left(\frac{T_0}{T}\right)^{3/2} \propto Z_{eff} \Rightarrow \qquad \frac{dI_>}{dt} = \frac{V}{L} - \frac{R_0}{L} I_{T_0}{}^{6/5} I_{p>}{}^{-1/5}$$

Imposing the smooth matching condition between the two *I* evolution equations and considering that the presence of dust influences the two parameters τ_b and Z_{eff}, a diagram of current evolution at start-up can be drawn.

[8] K. Hirano, Plasma Phys. **16** (1974) 1005.

Current ramp-up phase

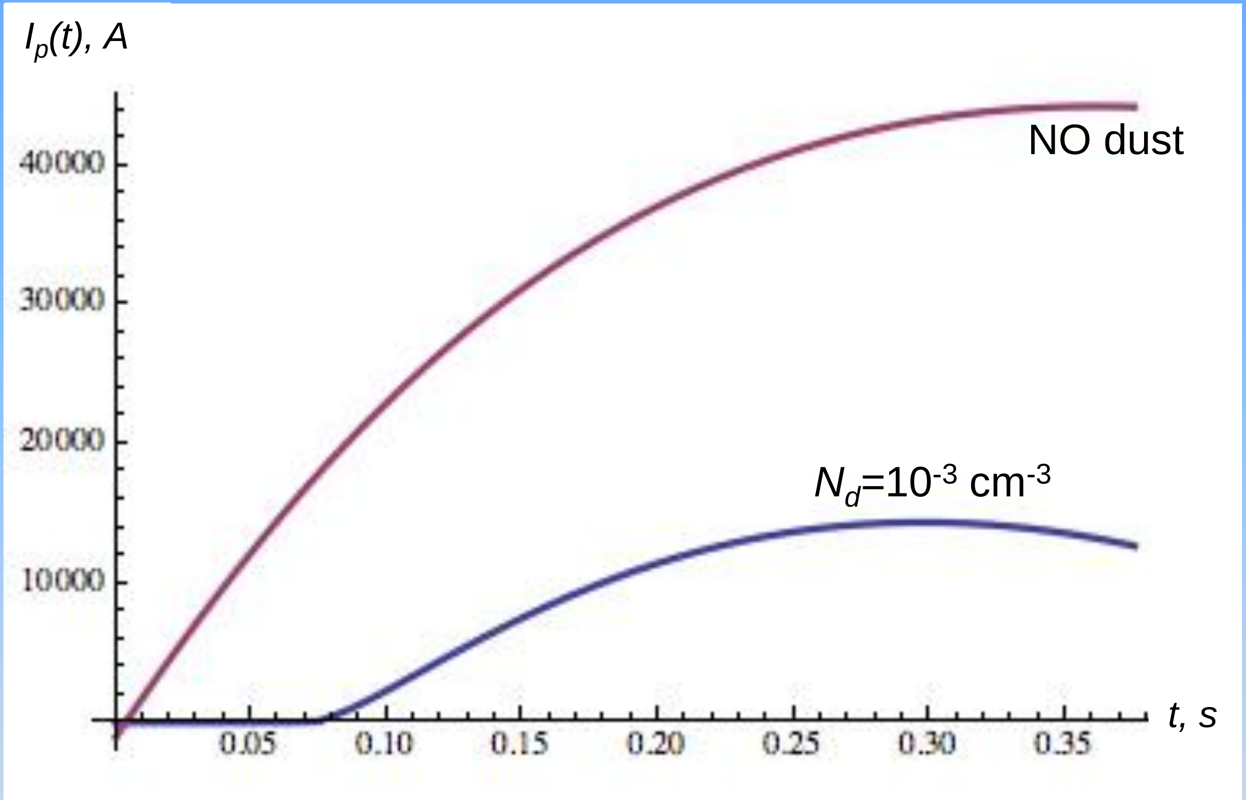

1. **First stage: presence of dust depletes free electrons ⇒ delay in start-up (τ_b increase).**
2. **Second stage: vaporization of dust ⇒ increases plasma resistivity ($\eta \propto Z_{eff}$) ⇒ lower I_P at plateau.**

Plot of plasma current build-up: I_p evolution through the breakdown phase to the inductive one, with thermally evolving resistance. **Blue line**: early transition from the Townsend avalanche phase to the inductive one with V_{loop} = 2.5V and R≅0.032Ω. **Red line**: case with no dust.

Dust evaporation at the beginning of I_p plateau

Big grains are not-magnetised, ion drag force too weak⇒**No deviation of dust trajectory**

Estimation of *Fe* grains lifetime (in ms) in 3 plasma scenarios (all with B=6T) by means of a model for dust-plasma interactions in strong magnetic fields (λ_{De}, $R_{Le} \ll R_d$) [9]. The model includes thermionic emission, secondary electron emission, electron and ion backscattering:

i- **clod scenario**: N_e=2 10^{19} m^{-3}, T_e=0.5ke*V*; *ii*- **medium scenario** N_e=5 10^{19} m^{-3}, T_e=1ke*V*; *iii*- **hot scenario**: N_e=8 10^{19} m^{-3}, T_e=1.5ke*V.*

Initial grains diameter →	20µm	50µm	100µm	200µm	500µm	
Cold scenario	0.15	0.46	1.16	3.12	12.6	*ms*
Medium	0.021	0.061	0.15	0.39	1.51	*ms*
Hot scenario	0.0067	0.020	0.048	0.12	0.47	*ms*

***Fe* grains lifetime**

Note: assuming a grain speed of 100 m/s, crossing the plasma volume in radial direction (~0.3m), it requires, at least, 3 ms.

⇒ **Increase of N_{Fe} and Z_{eff} leading to plasma power dissipation!!**

[9] L. Vignitchouk, S. Ratynskaia, P. Tolias, PPCF **59** (2017) 104002.

Dust evaporation at the beginning of the discharge

Fe grain diamiters, μm	N_{Fe}, m^{-3} (*single grain*)	Z_{eff} @ N_e=2x $10^{19}m^{-3}$ (*1 grain*)	Z_{eff} @ N_e=8x $10^{19}m^{-3}$ (*1 grain*)
20	$9.7x10^{13}$	1.00	1.00
50	$1.5x10^{15}$	1.05	1.01
100	$1.2x10^{16}$	1.39	1.10
200	$9.7x10^{16}$	3.80	1.76
500	$1.5x10^{18}$	17.6	9.25
1000	$1.2x10^{19}$	24.5	20.9

Hypotheses:

Dust: 100% of *Fe;*
Dust shape: spherical;
FTU Volume V: 2.07m^3;
Z_{Fe}=26 (!)

$$Z_{eff} = \frac{N_e Z_D^2 + N_{Fe} Z_{Fe}^2}{N_e Z_D + N_{Fe} Z_{Fe}}$$

N_{Fe} is not negligible compared to plasma density, even for the case of single grain !!!

Impact of remobilized dust *prior to* the beginning of plasma discharges: Summary

- **BREAKDOWN phase:**

Shifting of the Paschen's curve $\Rightarrow$ change of gas breakdown conditions.

- **RAMP-UP phase:**

- Depletion of free electrons $\Rightarrow$ delay in the start-up that could reach few 100s ms.
- Perturbation of plasma resistivity, through an increase of the Z_{eff}, $\Rightarrow$ lower I_p plateau level.

- **DUST EVAPORATION at first stage of full plasma:**

Evaporation of massive dust grains with high *Z* present in the plasma core upon a full plasma is established $\Rightarrow$ power loss and disruptions.

Conclusions

- Magnetic force ($F_B \propto \nabla B$) is the responsible for (magnetic) dust remobilization *prior to* plasma discharges in FTU;
- The average dust density, evaluated over several experimental campaigns, spans from **2 to 30x10^{-3}cm^{-3}** with dust size between **few 10's µm up to few mm**;
- The estimated dust density values are averaged on FTU campaigns, the actual value for a single shot **could change dramatically shot-by-shot**.
- Dust at start-up can have **dramatic effect on plasma start-up** phase;

Overall comments:

- FTU is a peculiar machine, nevertheless **magnetic dust has been found in several other machines** and could be a potential harmful.
- It is **difficult prove that discharge inhibition or disruptive events are caused by the presence of magnetic dust**, nevertheless the presence of mobilized magnetic dust *prior to* plasma discharges *is a matter of fact*!
- In the prospective to use steel components and RAFM[1] materials in ITER and future fusion power plants [10,11], the possible presence of magnetic dust in the device could be an issue. In fact ITER and future plants will be equipped with **superconductive coils and will have low loop voltage** for plasma breakdown and start-up.
- **Good news: Magnetic dust can be easily removed by means of a magnet mounted on a remote harm handling without break the vacuum!** ☺

[10] R.A Pitts, et al., J. Nucl. Mater. **463** (2015) 748.
[11] K. Sugiyama, K. Schmid, W. Jacob, Nucl. Mater. Energy **8** (2016) 1.

[1] RAFM= Reduced-Activation Ferritic-Martensitic material.

Thank you for your attention!

Authors acknowledges F. Ghezzi and G. Grosso for valuable discussion.

Backup slides

Preliminary examples of magnetic dust dynamic

Fe spherical particles trajectories during a B_t ramp-up from 0 to 5T
(hyp: mirror reflections on the walls; no dust adhesion forces included; only B_t present).

- work in progress -

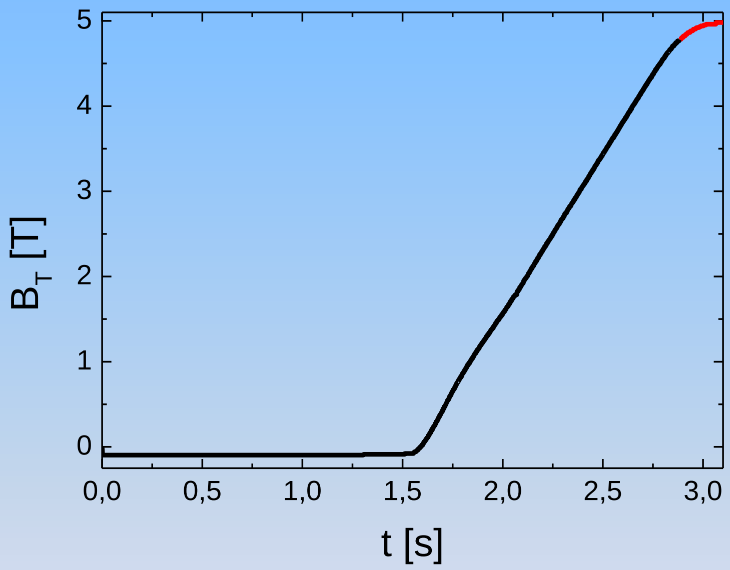

Toroidal field ramp-up timing.

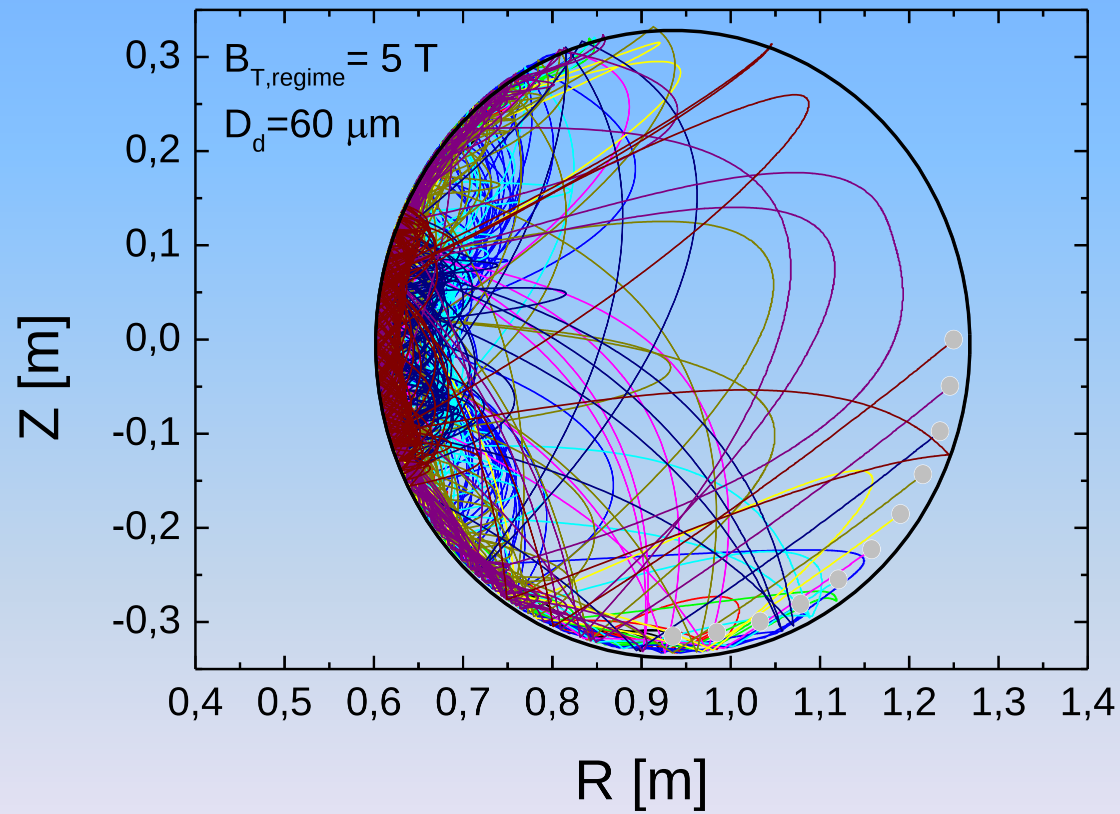

11 particles trajectories in a pure toroidal magnetic field.
Poloidal cross-section view.

Magnetic force components F_φ vs F_r

FTU poloidal cross section view with multi-pole magnetic field B(φ,r,z) map.

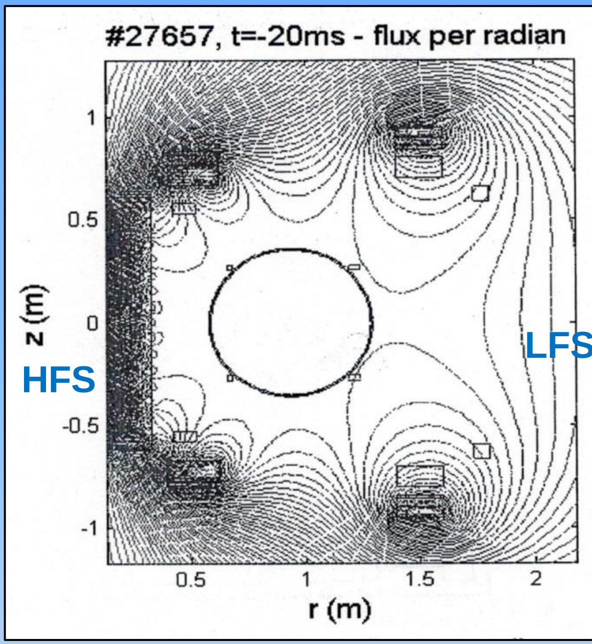

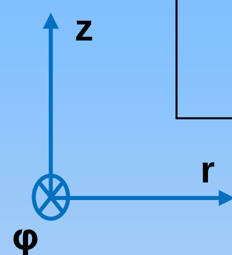

φ, toroidal direction.

$\boldsymbol{F}_{\nabla B} = \boldsymbol{\mu}\cdot\nabla\boldsymbol{B}$, $\boldsymbol{B} = B_r(r,z)\boldsymbol{e}_r + B_\varphi(r)\boldsymbol{e}_\varphi + B_z(r,z)\boldsymbol{e}_z \Rightarrow$

$$\begin{cases} F_r = \mu_r \dfrac{\partial B_r}{\partial r} + \mu_z \dfrac{\partial B_r}{\partial z} - \mu_\varphi \dfrac{B_\varphi}{r} \\ F_\varphi = \mu_\varphi \dfrac{B_r}{r} + \mu_r \dfrac{\partial B_\varphi}{\partial r} \\ F_z = \mu_r \dfrac{\partial B_z}{\partial r} + \mu_z \dfrac{\partial B_z}{\partial z} \end{cases}$$

Isolevel diagram of the rate F_φ / F_r

$$\frac{F_\varphi}{F_r} = \frac{\dfrac{B_r}{r} - \dfrac{B_\varphi}{r}}{\dfrac{\partial B_r}{\partial r} + \dfrac{\partial B_r}{\partial z} - \dfrac{B_\varphi}{r}}$$

with $\boldsymbol{\mu} \equiv \mu_{intrinsic}$ and $B_\varphi = \dfrac{B_{\varphi o} r_o}{r}$.

The two components are of the **same order of magniture!!**

Shot# 40688
t= -850ms

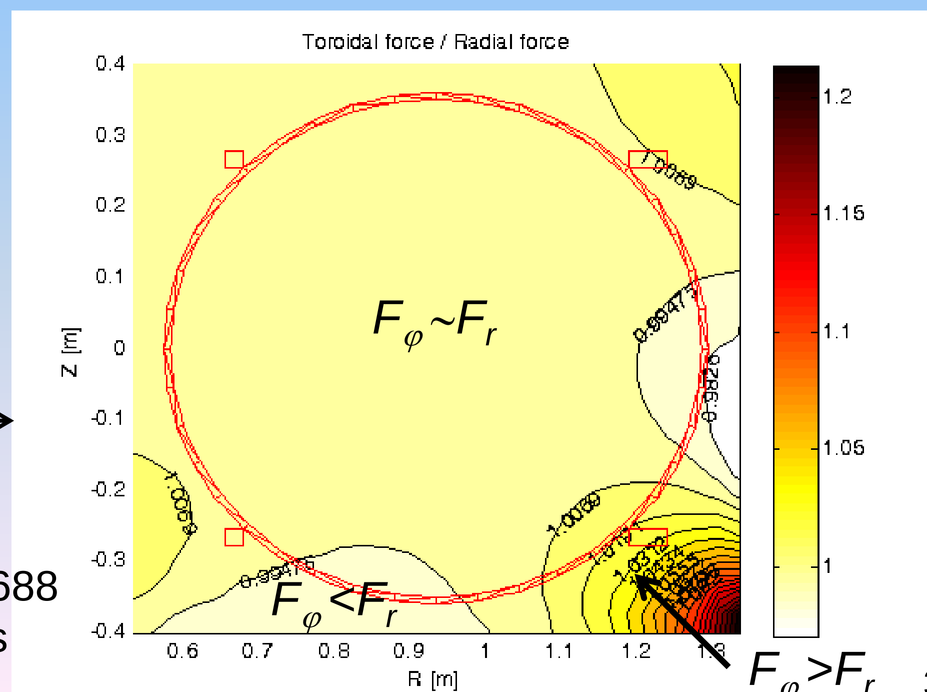

There are some evidences of disrupted discharges with presence of Fe lines in spectroscopy

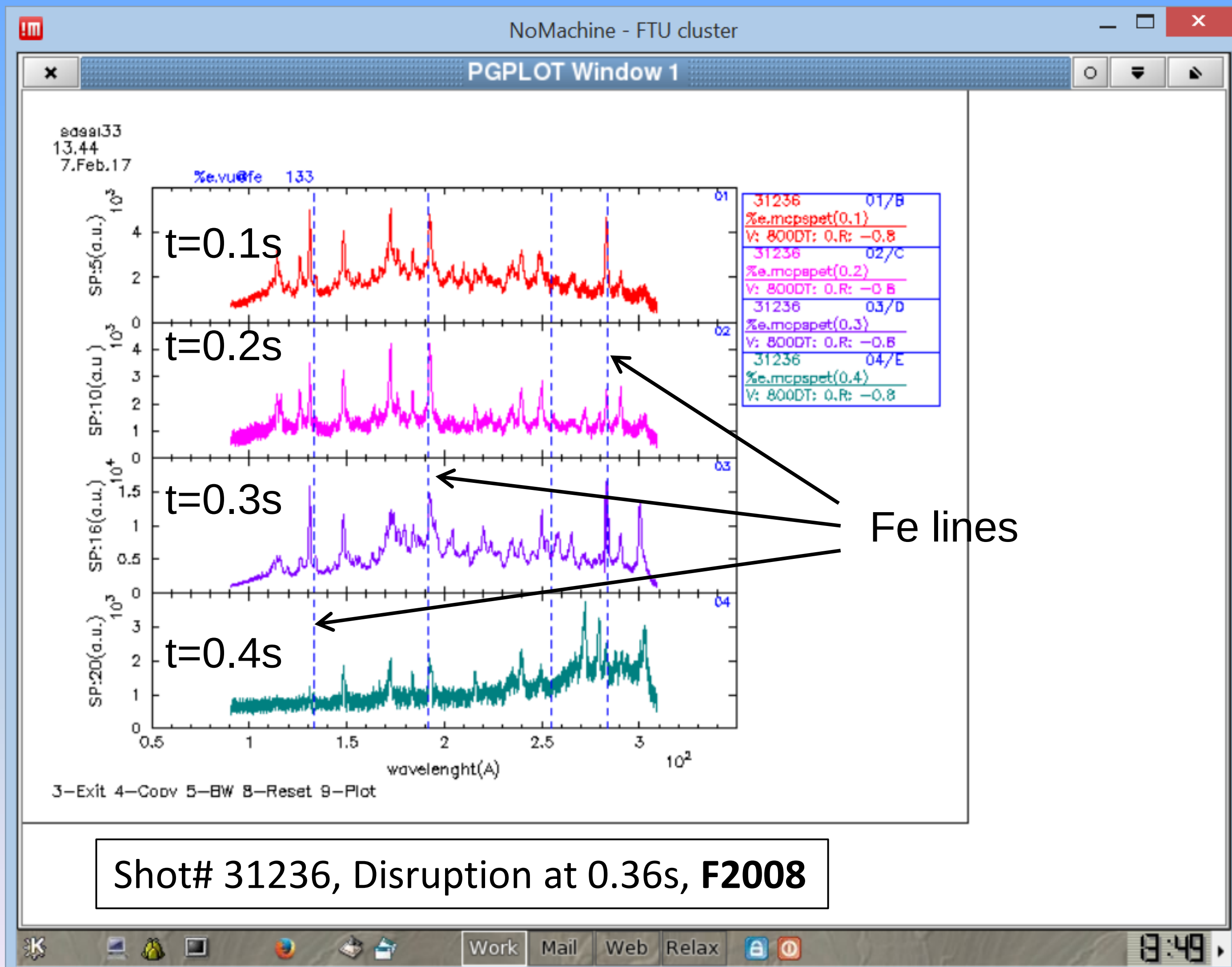

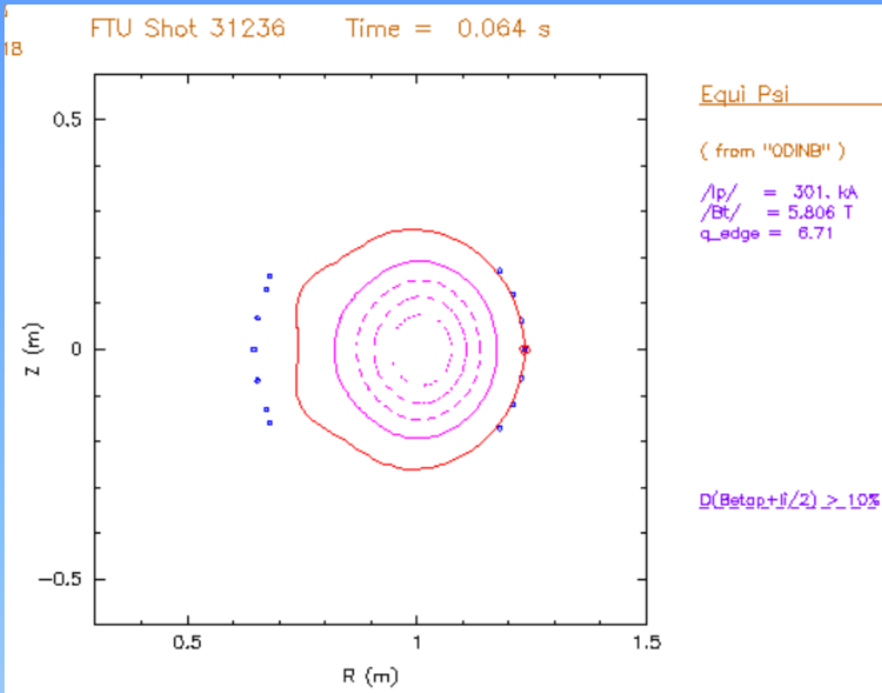

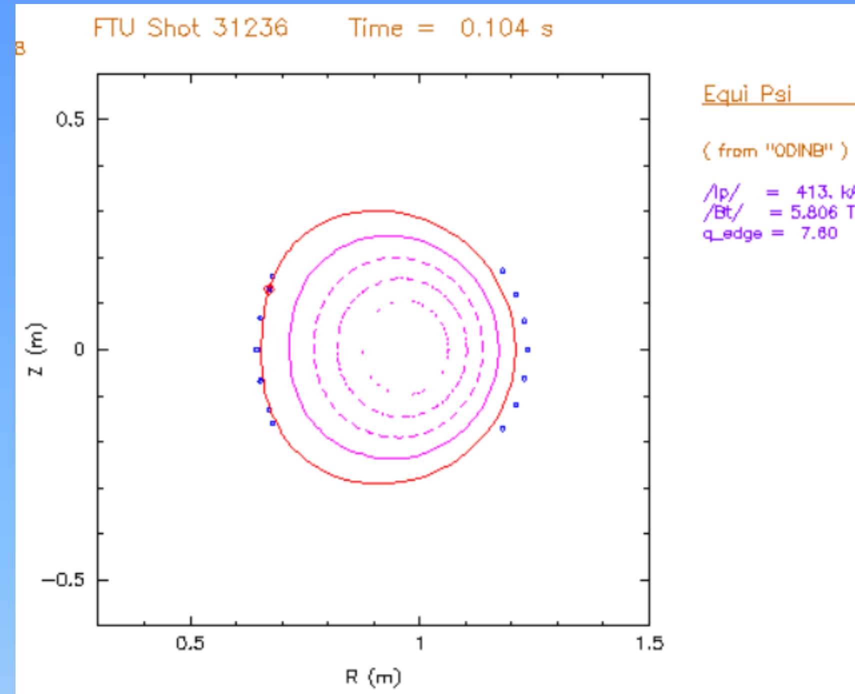

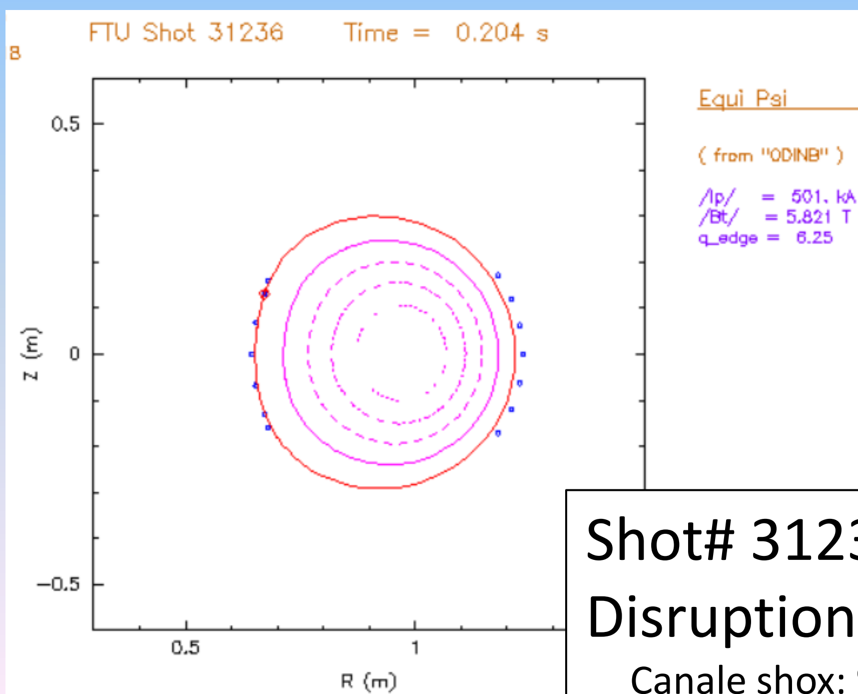

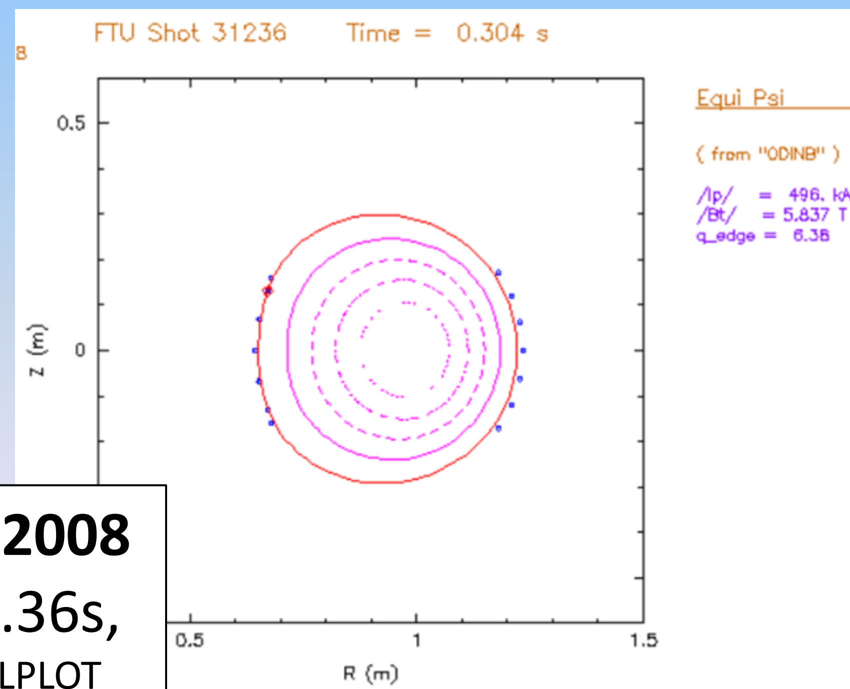

Shot# 31236, **F2008**

Disruption at 0.36s,

Canale shox: %E.EQLPLOT

Plasma column position:

Posizione verticale ($eqvz)

Posizione orizzontale $eqvr

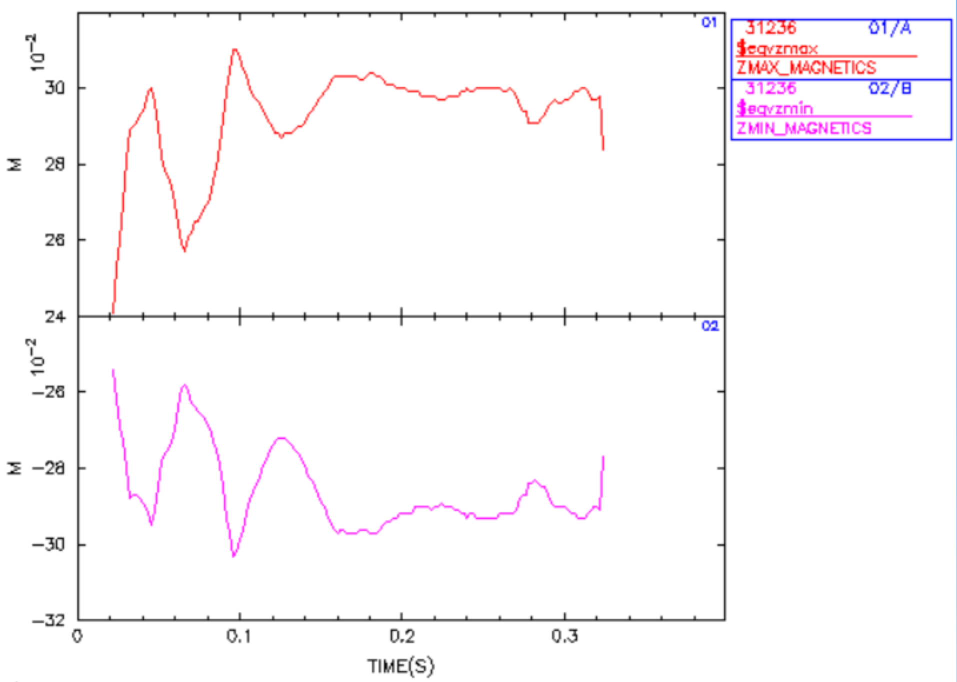

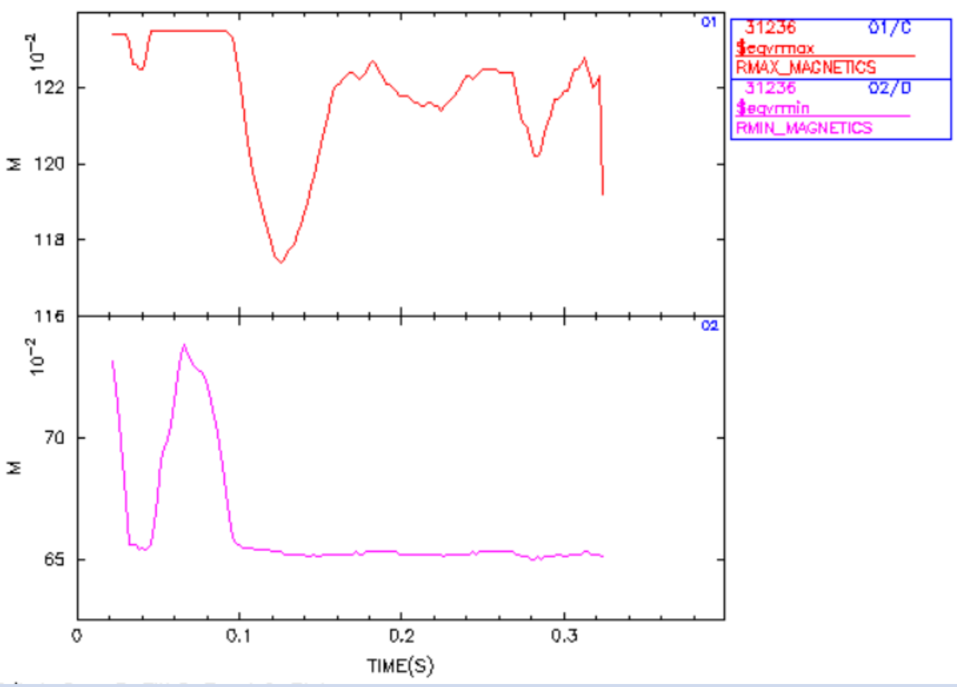

Shot# 31236, **F2008,** Disruption at 0.36s

Experimental campaign statistics in FTU

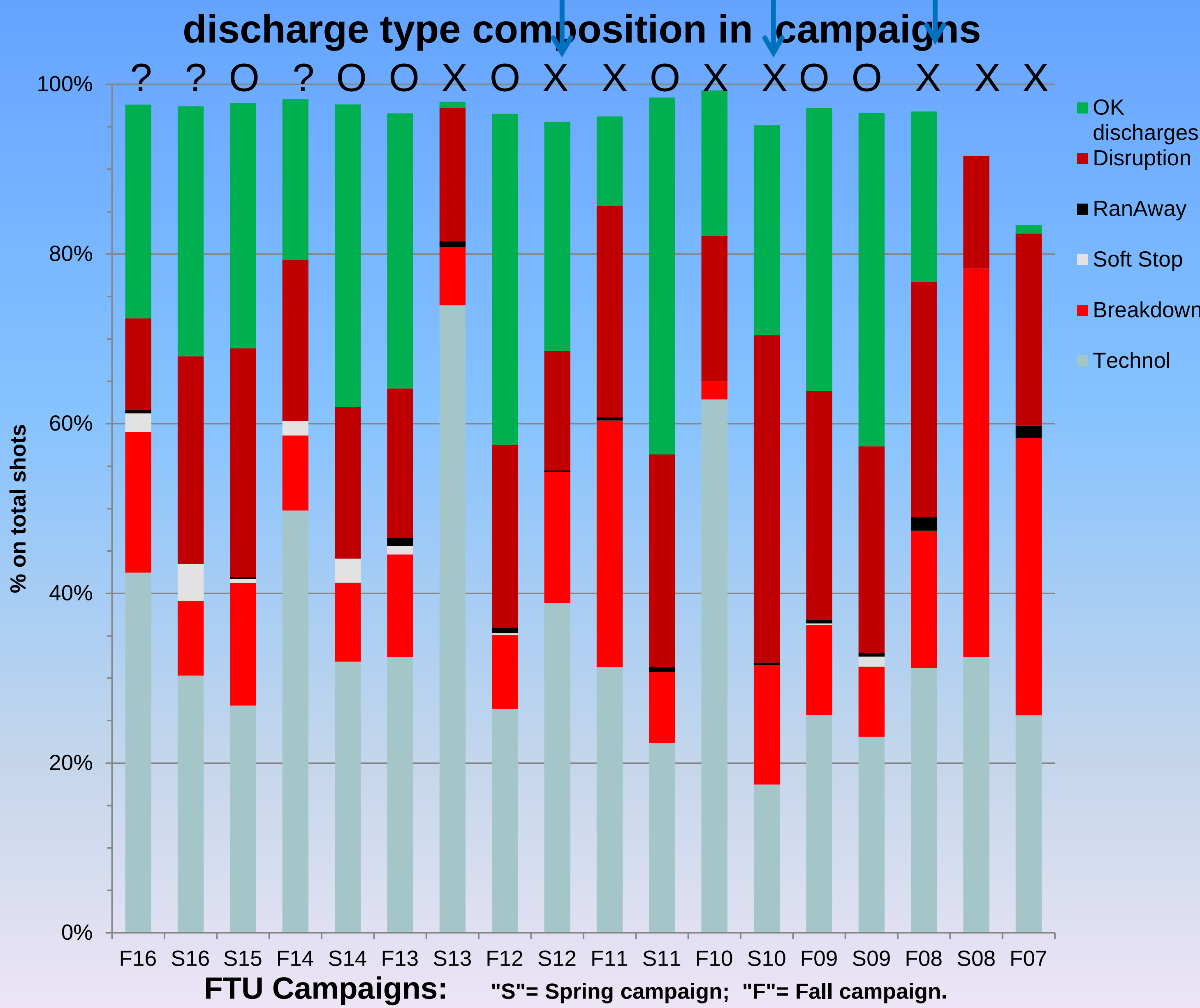

Discharges in camp:
F07: 199 only restart
S08: 83 only restart
F08: 439 only restart
S09: 1339
F09: 650
S10: 355 only restart
F10: 140 only restart
S11: 1032
F11: 265 No TS
S12: 589 only restart
(tech problems?)
F12: 895
S13: 146 No TS
F13: 1144
S14: 676
F14: 464
S15: 1244
F15: 78 No TS
S16: 465
F16: 464
Tot discharges: 10589

Ok: campaigns with high rate of «OK» and low of «BK»;

X: campaigns with low rate of «OK» and/or high of «BK»/»D».

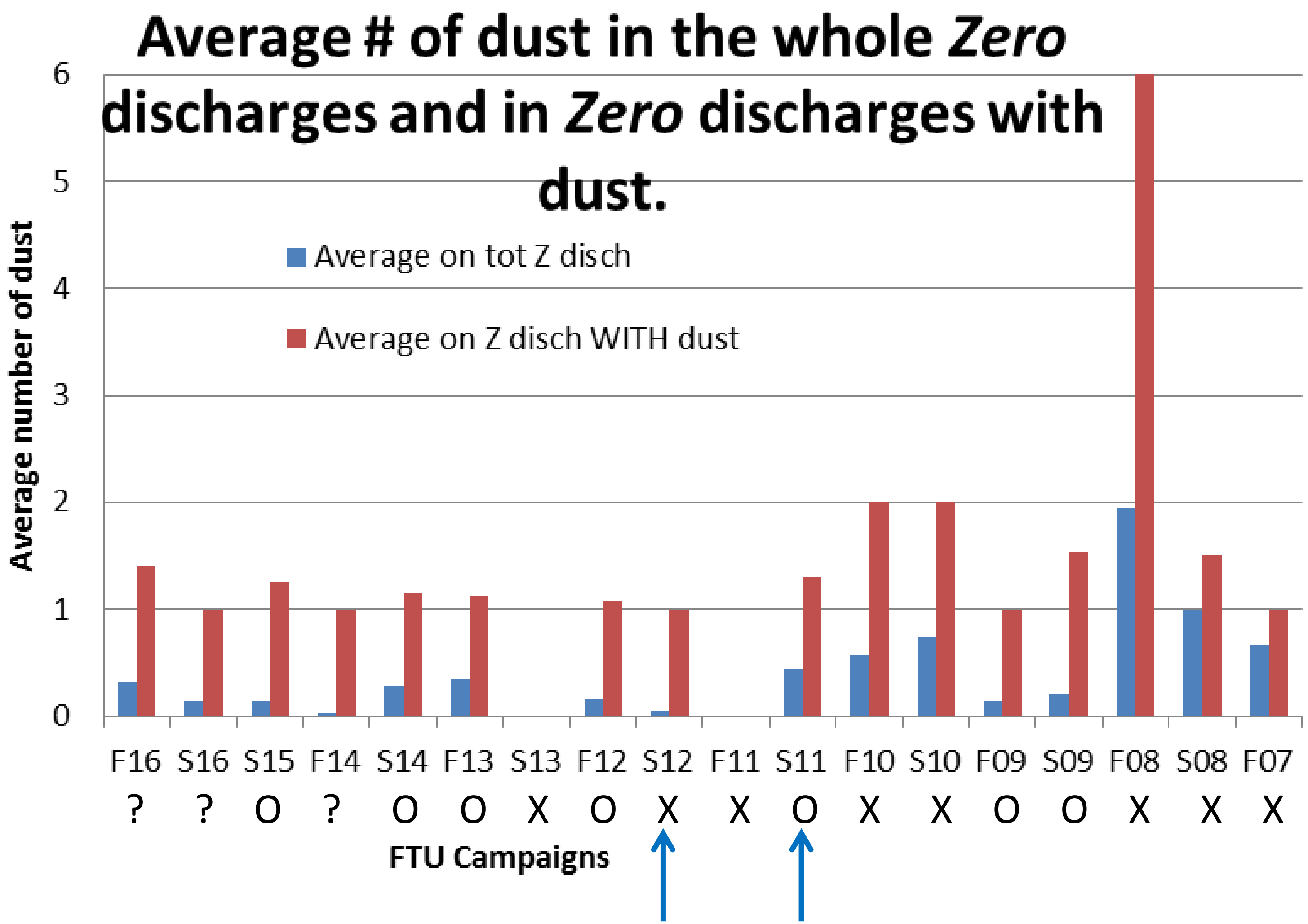

Zero dischs with dust vs *Zero* w/o dust:
F07: 2/3 only restart
S08: 2/3 only restart
F08: 6/19 only restart
S09: 13/95
F09: 7/49
S10: 6/16 only restart
F10: 2/7 only restart
S11: 27/79
F11: No TS
S12: 1/18 only restart (tech problems?)
F12: 12/82
S13: No TS
F13: 24/79
S14: 13/53
F14: 1/28
S15: 12/100
F15: No TS
S16: 5/36
F16: 5/22
Tot *Z* disch with dust: 138.

Ok: campaigns with low rate of average dust per Zero discharges;
X: opposite.

2014 Fall campaign

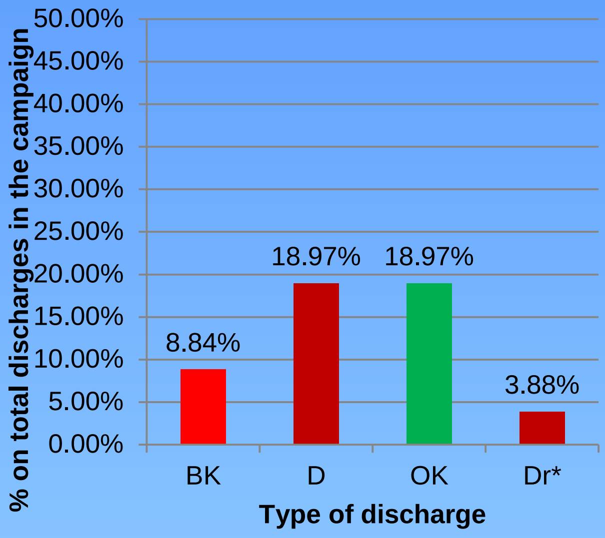

464

2014 Spring campaign

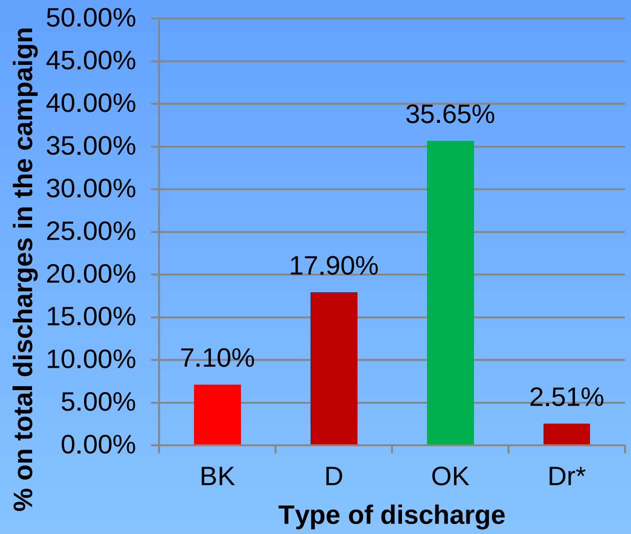

676

2010 Spring campaign

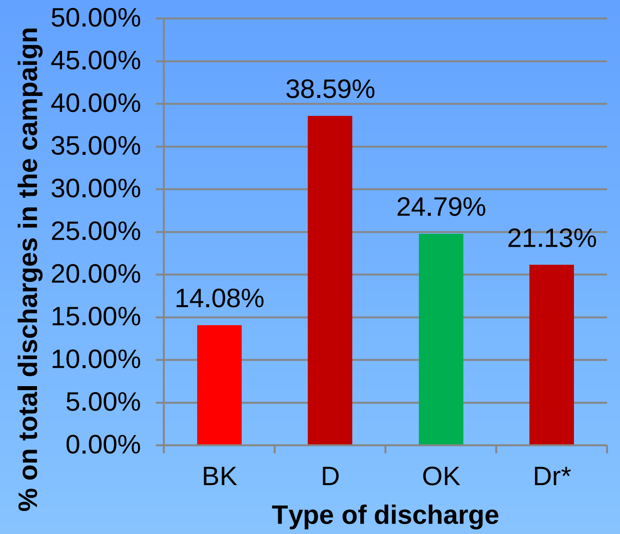

355

Blue: Total discharges in the campaigns. Ok: camps with low rate of D and BK dischs Vs OK; D=total # of disrupted dischs; Dr*=dischs disrupted <u>before Ip plateau </u>(t<200-300ms).

439

2008 Fall campaign

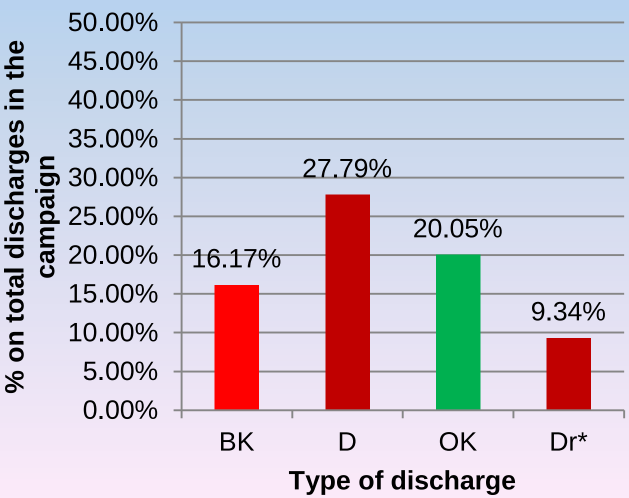

83

2008 Spring campaign

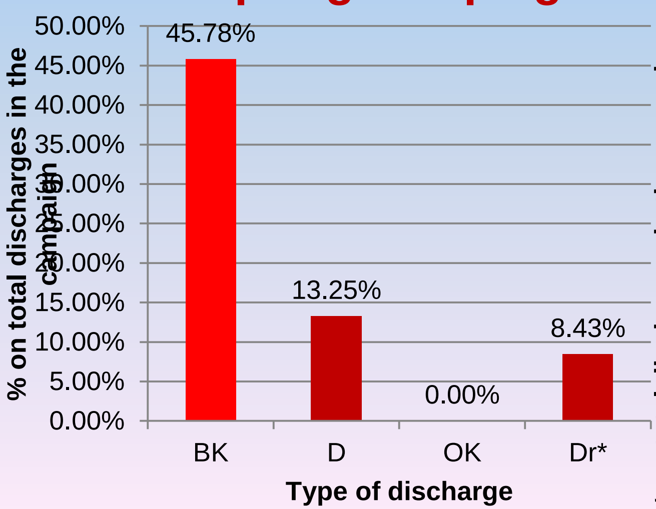

199

2007 Fall campaign

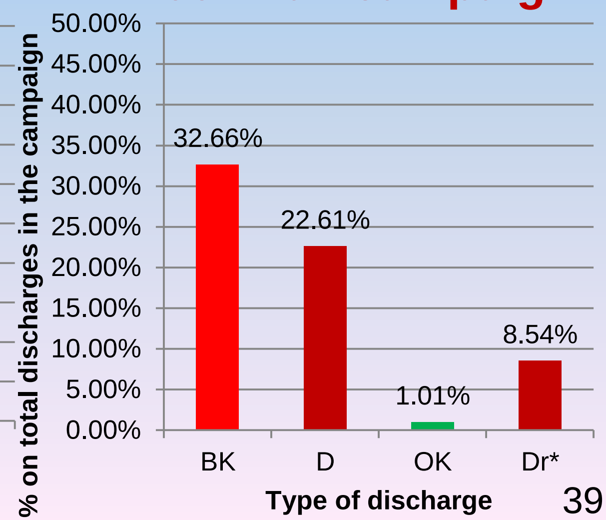

% of discharges with Dust vs no Dust (F2014)

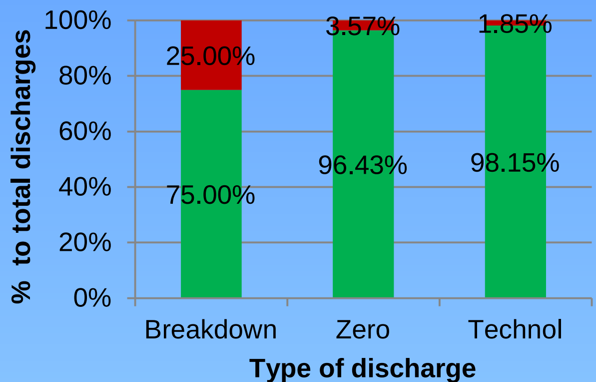

% of discharges with Dust vs no Dust (S2014)

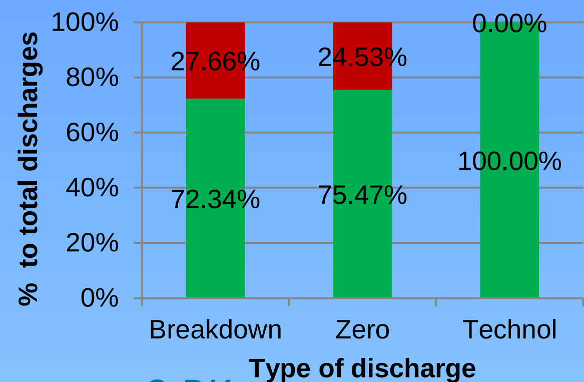

2 BK

% of discharges with Dust vs no Dust (S2010)

% of disch with dust = **61.3%**

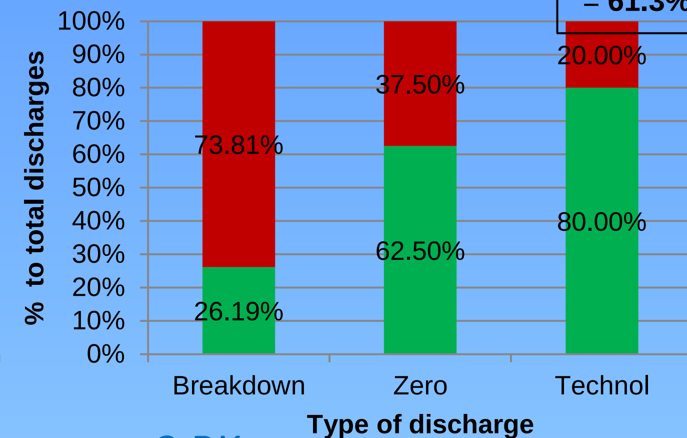

2 BK

Red: dischs with dust; Green: dischs without dust; Blue label: # dischs with dust at t=0.

Ok: camps with low rate of dust in BK, Zero, and T dischs.

% of discharges with Dust vs no Dust (F2008)

% of disch with dust

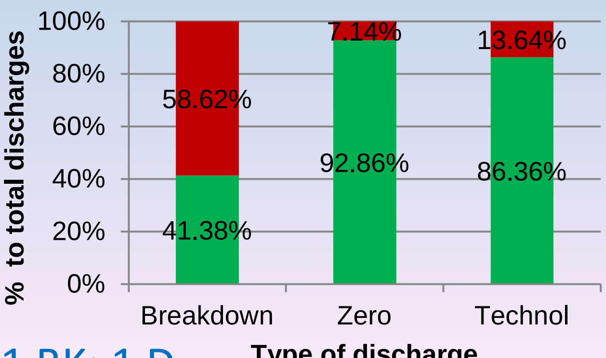

1 BK; 1 D

% of discharges with Dust vs no Dust (S2008)

% of disch with dust = **51.8%**

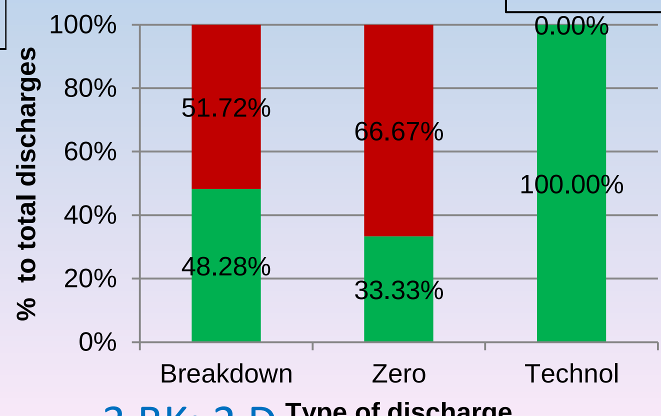

3 BK; 2 D

% of discharges with Dust vs no Dust (F2007)

% of disch with dust

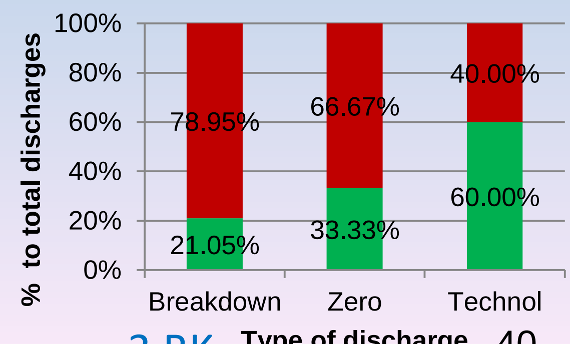

3 BK